ORIGINAL PAPER

Identifying Detrital and Diagenetic Minerals in Paleosols of the Illinois Basin

Julia A. McIntosh[ID] · **W. Crawford Elliott**[ID] ·
J. Marion Wampler[ID] · **Neil J. Tabor**[ID]

Abstract Phyllosilicates are hypothesized to be primarily of pedogenic origin in shallowly buried paleosols (≤3 km depth), regardless of the age of the paleosol. To test this hypothesis, this work evaluates the possible presence of detrital and diagenetic phyllosilicates in middle and upper Pennsylvanian paleosols, collected from three drill cores along a north–south transect in the Illinois Basin. The abundances of $2M_1$ muscovite, quartz, and K-feldspar are greater in a morphologically immature Protosol from the southernmost core; $1M_d$ illite and interstratified illite-smectite with R1 and R0 stacking orders are more abundant in the more mature Vertisols of the central and northern cores. K-Ar age values of multiple clay-size fractions from each paleosol averaged ~260 Ma in the northern core, 270 Ma in the central core, and 295 Ma in the southern core. While considering the complex tectonic and thermal history of the Illinois Basin, detrital minerals are more abundant in immature paleosols that experienced relatively greater maximum burial depths and thus greater sediment supply whereas illitization in more mature paleosols was probably initiated primarily during protracted burial diagenesis. As the present study found evidence for diagenetic and detrital minerals in clay-size fractions of shallowly buried, deep-time paleosols, caution is advised when using paleosol minerals for ancient climate and environment reconstructions.

Keywords Illite-smectite · K-Ar · Pedogenesis · Pennsylvanian · XRD

Present address of Julia A. McIntosh is Geology, Geophysics, and Geochemistry Science Center, U.S. Geological Survey, Denver, CO 80225, USA

J. A. McIntosh (✉) · N. J. Tabor
Roy M. Huffington Department of Earth Sciences, Southern Methodist University, Dallas, TX 75275, USA
e-mail: jmcintosh@usgs.gov

W. C. Elliott · J. M. Wampler
Department of Geosciences, Georgia State University, Atlanta, GA 30302, USA

Springer

Introduction

Illite is a type of 2:1 layer phyllosilicate mineral that is structurally and compositionally similar to muscovite except that it contains more Si, Mg, and H_2O but less Al and K (Grim et al., 1937; Guggenheim et al., 2006, 2007; Moore & Reynolds, 1997; Rieder et al., 1998). Illite may be a discrete phase or it may exist in the form of an interstratified phase such as illite-smectite (I-S), where the latter may contain variable abundances of topotactically stacked illite and smectite layers. Smectite can be transformed into I-S, where smectite is dehydrated, octahedral Al^{3+} substitutes for some

of the Si^{4+} in the tetrahedral sheet, Fe^{2+} and Mg^{2+} replace some of the Al^{3+} originally in the octahedral sheet, and anhydrous K^+ is preferentially fixed in the interlayer space over other exchangeable cations (Boles & Franks, 1979; Hower et al., 1976). Beginning with studies in the USA Gulf Coast, smectite illitization was thought to occur predominantly due to increased temperatures, high water:rock ratios, abundant aqueous K, and time associated with burial diagenesis (Boles & Franks, 1979; Hower et al., 1976; McCarty et al., 2008; Perry & Hower, 1970; Środoń, 1999b). On the other hand, smectite illitization may also be advanced under low-temperature surface conditions with cyclical wetting and drying (Eberl et al., 1986). It may also occur during iron redox cycling (Shen & Stucki, 1994), when structural iron is reduced chemically (Eslinger et al., 1979) or biologically (Dong et al., 2009). Lastly, I-S and illite may be detrital components of a clastic sedimentary rock (Eberl, 1984). Because no singular process produces I-S, methods beyond mineralogical characterization must be considered to ascertain the origins of I-S and illite in sedimentary rocks.

Phyllosilicate formation in soils occurs on the earth's surface under the influence of water-dominated weathering systems, such that the geochemical compositions of rocks interpreted to be fossilized soils, hereinafter referred to as paleosols, can be used to reconstruct ancient environments and climates (e.g. Savin & Hsieh, 1998; Sheldon & Tabor, 2009; Tabor & Myers, 2015). To be used as terrestrial paleoclimate proxies, phyllosilicates must have formed during episodes of pedogenesis in the past. There are two alternatives for the origins of phyllosilicates in paleosols: (1) inheritance as detritus before and/or during soil formation; and (2) formation during diagenetic or hydrothermal processes after soil formation (Curtis, 1985; Eberl, 1984; Nesbitt, 1992). Thus, if the geochemical and mineralogical signatures from phyllosilicates in paleosols are not characterized extensively, then geochemical effects spurred by sedimentary basin subsidence or uplift and/or hydrothermal alteration may be interpreted erroneously as signatures of ancient climate conditions.

The measurement of K and radiogenic ^{40}Ar are useful means of dating crystallization of muscovite, illite, and I-S (Bailey et al., 1962; Clauer, 2013). When detrital illite, or $2M_1$ muscovite, is present in the clay fraction, the K-Ar age of authigenic illitic material cannot be obtained directly. The measured amounts of the polytypes may be used to estimate the relative amounts of detrital and authigenic material in different size fractions, allowing age estimates for the two components to be derived from K-Ar age values of those fractions (Elliott et al., 2006; Grathoff & Moore, 1996; Grathoff et al., 2001; Pevear, 1999; Środoń et al., 2002). K-Ar age values of multiple size fractions of paleosol matrices are a function of the distribution of detrital (older than the paleosol), pedogenic, and diagenetic (younger than the paleosol) minerals. As a singular paleosol is probably a mixture of detrital, pedogenic, and/or diagenetic minerals, the K-Ar age value is not indicative of a specific event at that calculated time. Such a value reflects the ratio of the total radiogenic Ar to total K in a mixture, which may not be equal to the ratio of radiogenic Ar to K of any mineral component of the mixture. Much like K-Ar age values from clastic sedimentary rocks that have been diagenetically influenced (e.g. Bechtel et al., 1999; Elliott et al., 2006; Grathoff & Moore, 1996), K-Ar age values from paleosols should be viewed as averages, approximately (Środoń, 1999a), of the ages of diagenetic, pedogenic, and detrital minerals. The K-Ar technique has been used in studies of illite in paleosols, used more to discover information about the diagenetic history than for paleoclimate purposes (Lander et al., 1991; Mora et al., 1998).

The Illinois Basin (IB) is a tectonically stable cratonic basin which originated through rifting of the early Paleozoic Reelfoot rift system (Fig. 1; Buschbach & Kolata, 1990; Kolata & Nelson, 1990a,b). The IB contains a thick stratigraphic sequence of Carboniferous cyclothems the strata of which include marine units of shale and limestone, followed by nonmarine units of quartz-rich sandstones, shale, limestone, coal, and underclays (Fielding, 2021; Wanless, 1931; Weller, 1930, 1931; Willman et al., 1975). Cyclothems are interpreted to have formed from cycles of transgression and regression triggered by glacio-eustatic fluctuations (Cecil et al., 2014; Crowell & Frakes, 1970; Heckel, 1994, 2008; Montañez, 2022; Veevers & Powell, 1987; Wanless & Shepard, 1936). IB coals have been used for understanding ancient flora and thus reconstructions of Pennsylvanian paleoenvironments (e.g. DiMichele & Phillips, 1996; DiMichele et al., 2006; Phillips et al., 1974). More important to the present work, these coal beds are frequently underlain by an underclay. Due to the IB underclay's hackly and argillaceous matrices, lack of bedding, common rooting structures, and

⌘ Springer
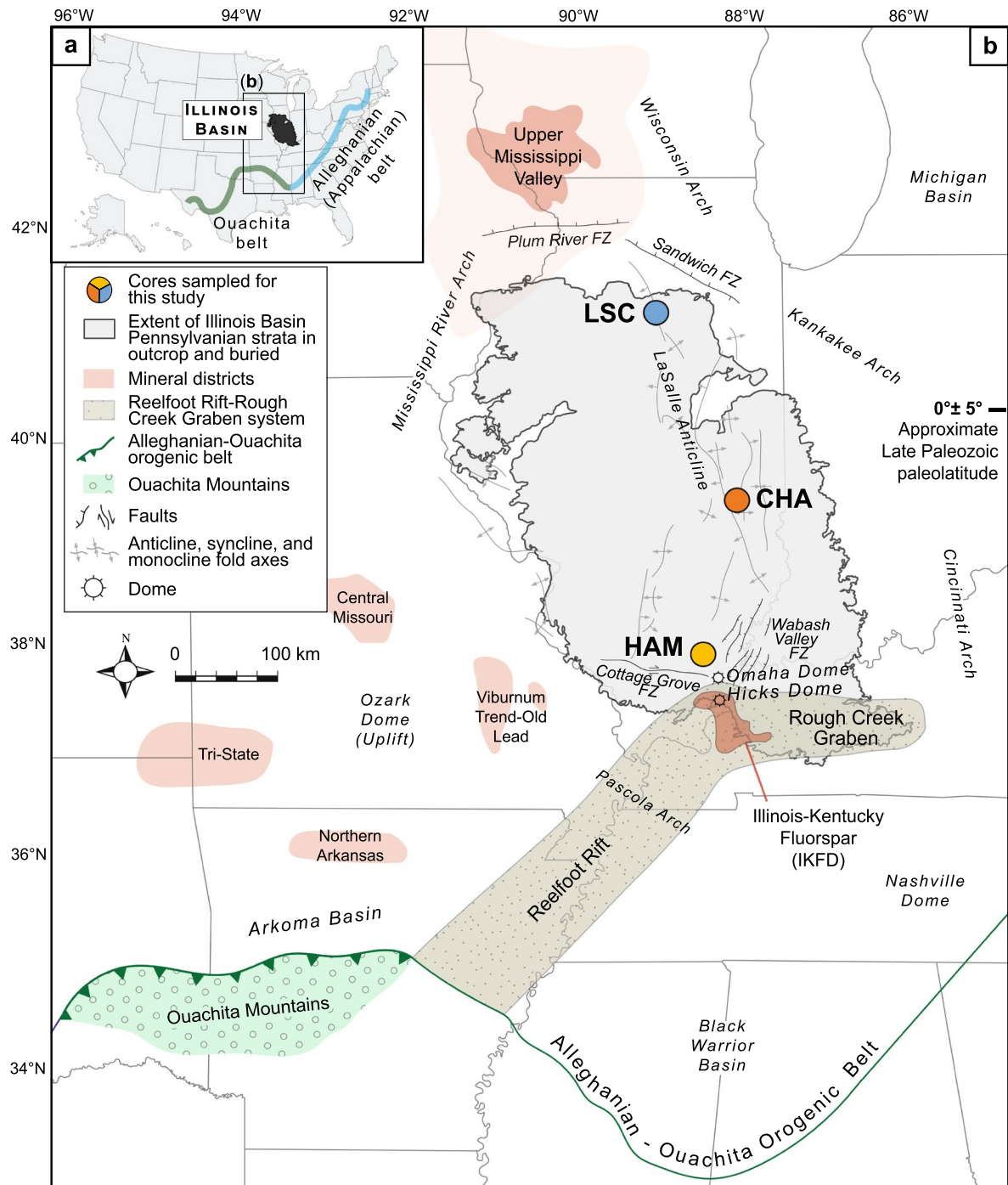
Fig. 1 Map of the Illinois Basin: **a** inset map of the Illinois Basin located in the midcontinent region of North America; the Alleghenian-Ouachita orogenies are noted in blue and green, respectively. **b** The extent of Pennsylvanian strata (both exposed in outcrop and buried) in the Illinois Basin (Rosenau et al., 2013a), surrounding arches and domes, a series of faults, fault zones (F.Z.), and minor folds (Nelson, 1995), and the Reelfoot Rift–Rough Creek Graben (Kolata & Nelson, 1990a) are shown. Mining or mineral districts of economic significance are shown in light red (Denny et al., 2008; Rowan & de Marsily, 2001). The cores sampled in the present study are the Lone Star Cement Company #TH-1 (LSC), the Illinois State Geological Survey #1 City of Charleston (CHA), and the American Coal Company Borehole 7510-20 (HAM). Paleolatitude information from Domeier et al. (2012)

morphologic structure and horizonization akin to modern soils, these underclays have been interpreted as paleosols (Grim & Allen, 1938; McIntosh et al., 2021; Rosenau et al., 2013a, b; Schultz, 1958).

Paleosols in Pennsylvanian strata of the IB have been identified as Vertisols, Calcisols, and Protosols with gleyed and/or calcic modifiers (Rosenau et al., 2013a), using the Mack et al. (1993) paleosol classification system. The characteristic clay-sized fraction of IB paleosols include the minerals I-S, illite, kaolinite, and chlorite (Elsass et al., 1997; Grim & Allen, 1938; Huddle & Patterson, 1961; McIntosh et al., 2021; Parham, 1963; Rimmer & Eberl, 1982; Rosenau et al., 2013a; Schultz, 1958). These paleosols contain evidence of pedogenic minerals (Hughes et al., 1985; Grim & Allen, 1938; Parham, 1963; Rosenau & Tabor, 2013; Rosenau et al., 2013a,b; Schultz, 1958; Weller, 1930; Worthen, 1866), that should be synformational with the paleosols and thus Middle–Late Pennsylvanian in age (315–299 Ma; Cohen et al., 2013; Davydov et al., 2010; Heckel, 2008; Schmitz & Davydov, 2012). IB paleosols also contain evidence for detrital minerals (Hughes et al., 1985; McIntosh et al., 2021; O'Brien, 1964; Parham, 1963), that may be from the Grenville (980–1300 Ma) and Appalachian (490–350 Ma) basement terranes (Kissock et al., 2018; Thomas et al., 2020) and possibly from reworked sediments of the Mississippian–Lower Pennsylvanian strata (359–315 Ma; Kissock et al., 2018; Lawton et al., 2021; Potter, 1963; Potter & Glass, 1958; Potter & Pryor, 1961; Thomas et al., 2020; Willman et al., 1975). Evidence of diagenesis in other Pennsylvanian units of the IB includes vitrinite reflectance of Pennsylvanian coal organic matter (Altschaeffl & Harrison, 1959; Barrows, 1985; Cluff & Byrnes, 1990; Damberger, 1971; Gharrabi & Velde, 1995; Schimmelmann et al., 2009), hydrothermal minerals in some Pennsylvanian coals (Cobb, 1981; Whelan et al., 1988), crystallization temperatures for some paleosol phyllosilicates that are too high to be Pennsylvanian paleotemperatures (Rosenau & Tabor, 2013), and highly illitic I-S in some Pennsylvanian paleosols (Elsass et al., 1997; McIntosh et al., 2021; Rimmer & Eberl, 1982) and clastic rocks (Moore, 2000, 2003). These studies are often spatially and stratigraphically finite and thus the influence of diagenetic alteration across the IB remains unclear.

The diagenetic alteration products in Pennsylvanian rocks of the IB may be attributed to basin-wide changes following the Pennsylvanian. During the formation and breakup of Pangea from late in the Permian until the Jurassic, tectonic activity in Laurentia led to reactivated faulting and rifting (Kolata & Nelson, 1990a). High vitrinite reflectance values from the Pennsylvanian coals and fluid inclusions from sphalerites in these coals have led to an estimated maximum burial depth of the IB by 1–3 km of sediment in and after the Permian that was later uplifted and eroded (Cobb, 1981; Damberger, 1971). Lamprophyric, or ultrapotassic, igneous intrusions in the Illinois Kentucky Fluorspar District (IKFD; Fig. 1) are thought to have formed from alkaline ultramafic magma sourced from the lower crust (Bradbury & Baxter, 1992; Kolata & Nelson, 1990a) or upper mantle (Fifarek et al., 2001). Geochronologic data of minerals from these intrusions in the IKFD indicate crystallization of igneous minerals in the Middle Permian (~270 Ma; Denny, 2005; Fifarek et al., 2001; Reynolds et al., 1997; Snee & Hays, 1992). Moreover, there is later evidence for hydrothermal fluid migration events in the IB following the Permian magmatism, and hypothesized mixing between magmatic fluids and basin brines (Plumlee et al., 1995), that may have triggered critical mineral formation and mineral alteration in the IKFD in the Permian (Chesley et al., 1994; Lu et al., 1990) and possibly the Jurassic (Brannon et al., 1997; Ruiz et al., 1988; Symons, 1994).

The aim of the present investigation was to identify the K-bearing minerals, mica polytypes, and K-Ar age values of clay-size fractions of IB paleosols sampled from three cores of middle and upper Pennsylvanian strata. This study builds upon the findings of McIntosh et al. (2021) by providing insights into the different generations of minerals in IB paleosols in order to assess the influence of non-pedogenically formed minerals on the bulk geochemistry of paleosol matrices. This work highlights the necessity of performing a comprehensive geochemical characterization of phyllosilicates from deep time paleosols combined with an examination of the sedimentary basin's history prior to utilizing paleosol minerals for reconstructions of ancient climates and environments.

Materials and Methods

Sampling Core

Paleosol samples from strata near the Desmoinesian–Missourian (North American Series) boundary

were collected from cores stored at the Illinois State Geological Survey Core Repository in Champaign, Illinois, USA. Three cores examined for this study are the Lone Star Cement Company #TH-1 (LSC), the Illinois State Geological Survey #1 City of Charleston (CHA), and the American Coal Company Borehole 7510-20 (HAM; Figs 1, 2; Table 1). One paleosol from each core was collected from the middle and upper Pennsylvanian (Desmoinesian) Shelburn Formation, near the Danville coal, Athensville coal, and Exline and West Franklin limestone members (Fig. 2). Also, one paleosol was collected from each core from the upper Pennsylvanian (Missourian) Bond Formation, near the Fairbanks coal, the Flat Creek coal, and the Reel and Hall limestone members (Fig. 2). Paleosols were retrieved from depths from 4.5 to 295.6 m (Table 1). Paleosols were separated into horizons, described using established criteria (Retallack, 1988; Tabor et al., 2017), and classified into one of nine orders (Mack et al. 1993). The samples were collected from paleosols identified by Rosenau et al. (2013a) and McIntosh (2018) as having calcic, vertic, and gleyed features, where five are Vertisols and one is a gleyed Protosol (Table 1). Approximately 50 g of the classified paleosols were sampled for mineralogical and geochemical characterization.

Laboratory Preparation

Each paleosol was partially disaggregated by lightly crushing in a mortar and pestle, suspending in deionized water, and further disaggregated using an ultrasonic agitation bath. Each of the six crushed paleosols was treated to remove non-clay cementing minerals from the mixture. The removal of cements was achieved by treatment with: (1) 10% acetic acid to remove calcite; (2) sodium citrate-bicarbonate-dithionite solution to remove secondary iron (oxyhydr)oxides; and (3) 30% H_2O_2 solution to remove organic matter (Jackson, 2005; Sheppard & Gilg, 1996). Using centrifugation, the <2.0, <0.2, and <0.1 μm equivalent spherical diameter clay-size fractions were isolated from each treated paleosol sample (Jackson, 2005) for a total of 18 subsamples. Each fraction was then divided into two portions for mineralogical and K-Ar geochronological analyses. All chemicals used for pretreatment were purchased from the supplier VWR (Radnor, Pennsylvania, USA).
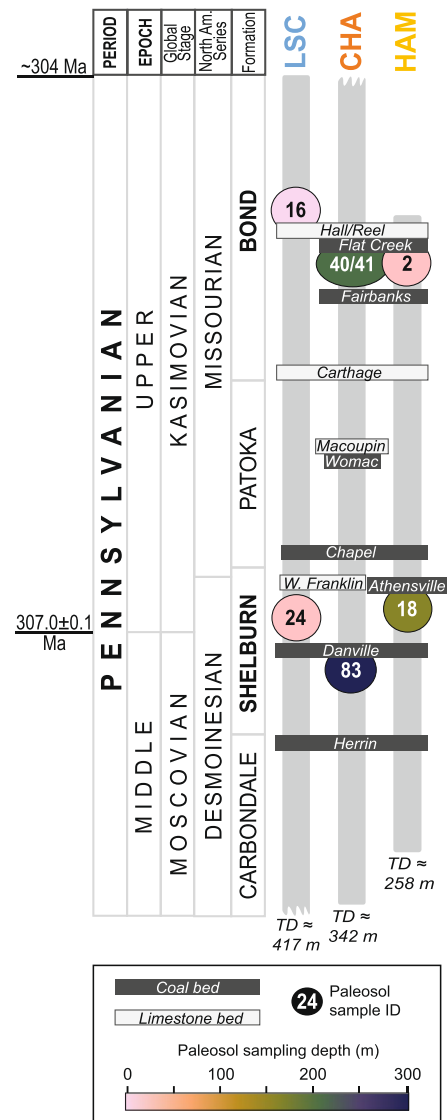
Fig. 2 Pennsylvanian stratigraphy of the Illinois Basin and points of sampling. Sample numbers for each core are denoted in ovals that are color coded to represent sampling depth. Important reference coals and limestones are noted. Numerical ages are from Cohen et al. (2013). TD = total depth. See Fig. 1 and Table 1 for more information on sample identifiers

Mineral Characterization using XRD

For each of the three size fractions prepared from each sample, the first portion was allocated to X-ray diffraction (XRD) analysis by preparing: (1) oriented smear slides; and (2) standard powder mounts.

Table 1 Sample details

Sample ID	Core latitude (°N)	Core longitude (°W)	North American Series	Formation	Paleosol type	Depth (m) [a]
LSC-16	41.287	-89.039	Missourian	Bond	calcic Vertisol	4.5
LSC-24			Desmoinesian	Shelburn	calcic Vertisol	35.4
CHA-40/41	39.499	-88.205	Missourian	Bond	gleyed calcic Vertisol	203.1
CHA-83			Desmoinesian	Shelburn	gleyed Vertisol	295.9
HAM-2	37.885	-88.606	Missourian	Bond	gleyed calcic Vertisol	20.5
HAM-18			Desmoinesian	Shelburn	gleyed Protosol	172.2

[a]Depth of sample from the surface

Oriented slides were prepared by adding suspended clay fractions to filter membranes (Kinter & Diamond, 1956); then the clay fractions were transferred to glass slides. Standard powder mounts were prepared by drying the suspended sample at 25°C, sieving the sample into a sample holder to distribute the powder randomly, and using a glass slide to pack the sample (or flatten the upper surface). All XRD analyses were performed using an Ultima III X-ray Diffractometer (Rigaku, Tokyo, Japan) at Southern Methodist University, using Cu-$K\alpha$ radiation. Operating conditions included a tube voltage of 40 kV, a tube current of 44 mA, a divergence slit of 2/3°, a receiving slit of 2/3°, and a fixed sample holder.

Three sets of oriented aggregates were prepared by: (1) air drying, (2) ethylene glycol solvation in a bell jar overnight at 60°C; and (3) heating to 500°C for 2 h. Oriented-aggregate slides were scanned over a range of 2 to 30°2θ with a step size of 0.01°2θ and a 1 s count time per step. The standard powder mounts were first heated to 550°C to prevent kaolinite from interfering in the mica diffraction patterns, specifically with the band at ~2.558 Å (Brindley, 1961), and then scanned over a range of 16 to 38°2θ with a step size of 0.025°2θ and a 30 s count time per step (similar to methods in Elliott et al., 2006; Grathoff & Moore, 1996). Though mineralogy is generally interpreted from XRD scans between 2 and 70°2θ, we instead acknowledge the work of previous mineral characterizations of IB paleosols (e.g. Rosenau et al., 2013a) and focus on characterizing K-bearing mineral phases to inform our K-Ar age values. Minerals were identified using the XRD pattern processing software *JADE* and *ClaySIM* (MDI, Livermore, California, USA).

Stacking orders of I-S were determined using the results from the XRD analyses of ethylene glycol-solvated oriented-aggregate slides. Ordering in the mineralogical sense is dependent on the number of interactions between neighboring layers in a phyllosilicate and the existence of an XRD-identifiable repetitive relationship(s), or interaction, of crystallographic form across the (001) axis (Reynolds, 1980). Reichweite (R) is a term used to describe ordering types (Jagodzinski, 1949), where R0 describes random interstratification and R1 and R3 correspond to ordered short-range and ordered long-range interstratification, respectively. The R0 stacking order was identified based on the presence of a peak at ~17 Å on the glycol-solvated oriented mounts. The R1 stacking order was identified based on the presence of the peak at ~13.5 Å on the glycol-solvated oriented mounts, wherein the superlattice peak was not observed at ~27 Å. The R3 stacking order was identified based on the peak being between 10 and 12 Å on the glycol-solvated oriented mounts (Hower, 1981).

Discrete muscovite and illite polytypes were identified from observed diffraction peaks and their *d* values of the standard powder mounts. Peak areas were determined using *JADE*. The percentage of the $2M_1$ polytype was determined from the area of the $2M_1$-specific reflection at 3.00 Å divided by the area of the 2.58 Å band (from ~2.55 to 2.59 Å), in a formula from Table 3 of Grathoff and Moore (1996). No $1M$ specific reflections at 3.66 and 3.07 Å were observed, so the remaining abundance is understood to be of the $1M_d$ polytype, the disordered form of the $1M$ polytype.

K-Ar Apparent Age Measurements

The second portion of each separated size fraction was used for the K-Ar work performed at the K-Ar Geochronology Laboratory at Georgia State

University (GSU). The K-Ar age values of three size fractions were determined for each of six paleosol samples. Four size fractions, LSC-16 <0.2 μm, LSC-24 <0.2 μm, CHA-83 <0.1 μm, and HAM-2 <2.0 μm were analyzed twice while CHA-40/41 <2.0 μm was analyzed three times to assess reproducibility and error. This resulted in a total of 23 analyses for K and Ar isotopic characterization.

To determine an age value, the potassium and radiogenic argon-40 contents of a single test portion of air-dried clay were measured by procedures very similar to those used for K-Ar measurements of glauconite concentrates and described by De Man et al. (2010). Briefly, ~30 mg of each pretreated and dried clay fraction was encapsulated in copper foil. The entire set of capsules was placed in the argon-extraction line and held under vacuum overnight. Then, each capsule was heated, in sequence, by an external wire-wound resistance heater for 10 min at ~1000°C. The extracted argon was diluted isotopically with a known amount of virtually pure ^{38}Ar (Universität Bern, Switzerland) added when the heating began. The mixture of Ar isotopes was purified by cold-trapping and reaction with hot titanium to remove condensable and reactive gases, and its isotopic composition was measured using a MS-10 mass spectrometer (Associated Electrical Industries, Manchester, England) at GSU. Pellets of the interlaboratory reference glauconite, GL-O (Odin et al., 1982), were also analyzed via the procedures used for the clay-sized fractions. The amount of ^{38}Ar added was determined by calibration with the interlaboratory reference biotite LP-6 Bio (Engels & Ingamells, 1977).

After retrieval from the Ar-extraction line, each copper capsule, with the enclosed solid, was digested in a closed fluorocarbon container by a 10:3 mixture (by mass) of concentrated HF and HNO$_3$ heated at ≤100°C. After digestion, the liquid was evaporated and the remaining solid was then dissolved in a carrying solution composed of 0.01 mol/kg CsCl and 0.1 mol/kg HNO$_3$. K concentrations in test solutions of dissolved digestate were measured with a Perkin Elmer Model 3110 atomic absorption spectrophotometer (Norwalk, Connecticut, USA) against reference solutions prepared from standard KCl (SRM-999, National Institute of Standards and Technology, Gaithersburg, Maryland, USA) and confirmed as accurate by measurement of K in a solution prepared

from LP-6 Bio at GSU. K-Ar apparent ages were calculated using the ^{40}K decay constants and the isotopic abundances for K-Ar geochronology listed by Steiger and Jäger (1977). The uncertainties of the K-Ar apparent ages were calculated for the 95% confidence level, or 2σ. See Supplementary Material 1 for a workbook with K-Ar data and calculations. Reagents used at GSU were purchased from Fisher Scientific (Waltham, Massachusetts, USA).

## Results

Paleosol Minerals and Mica Polytypes

X-ray diffraction patterns collected from air-dried, oriented aggregates (Figs 3, 4, and 5) indicated significant peaks at ~12.71 and 12.00–10.50 Å corresponding to I-S. XRD patterns of oriented aggregates solvated with ethylene glycol yielded peaks at ~30, 13.13–11.50, ~9.56, and ~5.24 Å (Figs 3, 4, and 5) associated with the expansion of I-S. Peaks at ~10.00, 5.00, and 3.35 Å correspond to discrete illite or muscovite. Peaks at ~7.14 and 3.58 Å correspond to kaolinite. Peaks at ~14.36, 7.14, 4.72, and 3.53 Å correspond to chlorite. Peaks at ~4.26 and 3.35 Å correspond to quartz. Peaks at ~4.22, 3.31, and 3.25 Å correspond to K-feldspar. Finally, XRD patterns from heated oriented aggregates yielded collapsed peaks at 7.14 and 3.58 Å associated with kaolinite and shifts of I-S peaks to 10 and 5 Å (Figs 3, 4, and 5). Peaks at ~4.50 Å are associated with mica, illite, and kaolinite, though not their basal spacings (Brindley & Brown, 1980), and thus can be a sign of improper preparation of oriented slides. The peak ~4.50 Å exists primarily in the coarsest size fraction rather than finer fractions (Figs 3, 4, and 5) and does not, therefore, interfere with I-S characterization.

On XRD patterns collected from slowly scanned, standard powder mounts heated to 550°C and scanned from 16 to 38°2θ, significant peaks occur at ~5.00, 4.52, 3.74, 3.50, 3.35, 3.21, 3.04, 3.00, 2.80, and 2.58 Å (Figs 6, 7 and 8). These diffraction peaks correspond to discrete illite or muscovite. Peaks at ~3.53, 2.83, 2.54, 2.48, 2.44, and 2.39 Å correspond to chlorite. Peaks at ~4.26 and 3.34 Å correspond to quartz. Peaks at ~4.22, 3.77, 3.31, 3.28, 3.24, and 2.90 Å correspond to K-feldspars. Peaks at ~3.58 and
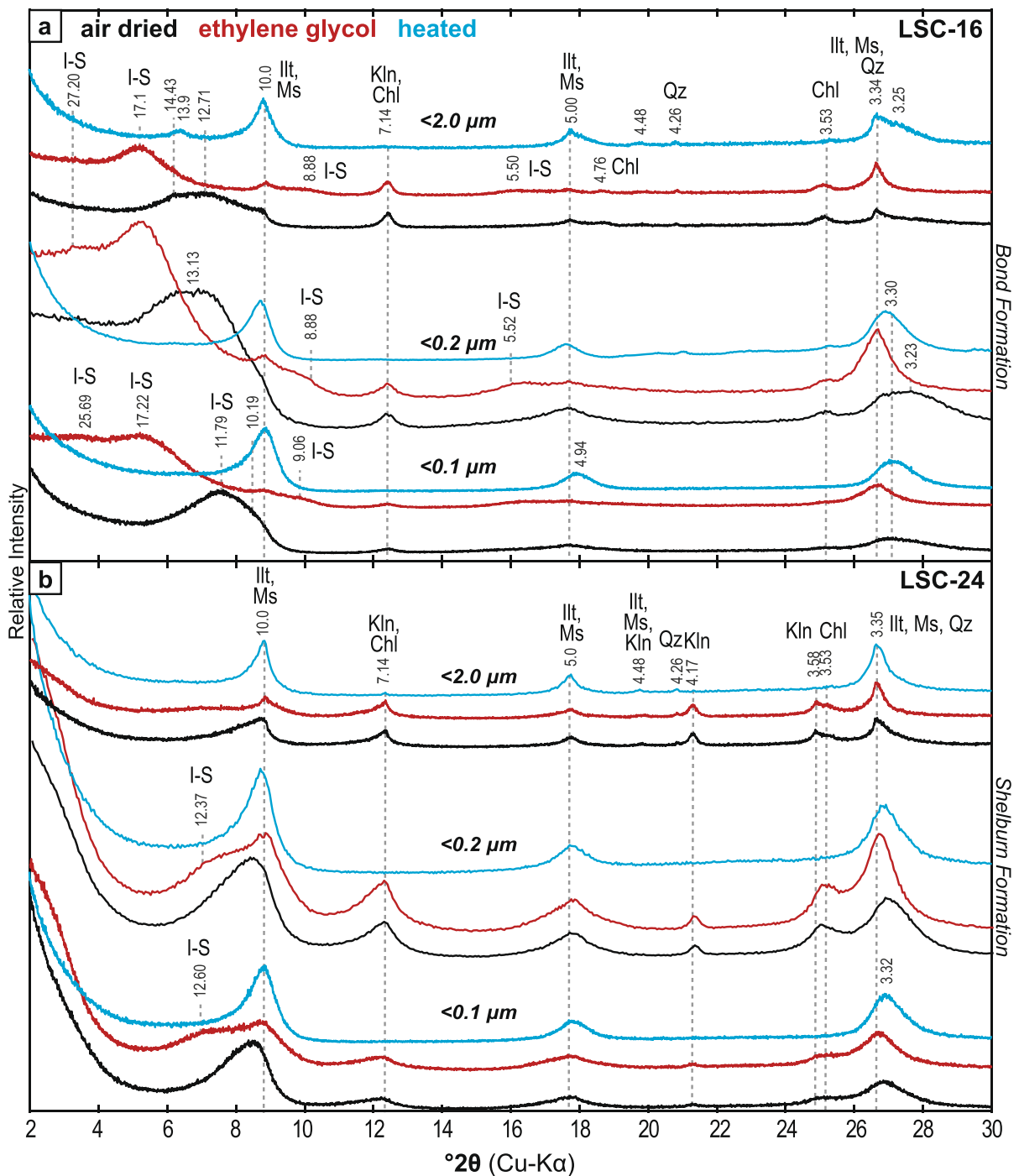
Fig. 3 XRD patterns of oriented aggregates of clay-sized fractions from LSC paleosol matrices for identification of minerals. Patterns for air-dried, ethylene glycol-solvated, and heated (to 500°C) samples are shown for each size fraction. Interplanar spacing values, d_{hkl} (Å), are noted vertically. Abbreviations of minerals are noted near d values and follow Warr (2020), such that Ilt = illite, Ms = muscovite, I-S = mixed-layer illite-smectite, Kln = kaolinite, Chl = chlorite, Qz = quartz, Kfs = K-feldspar
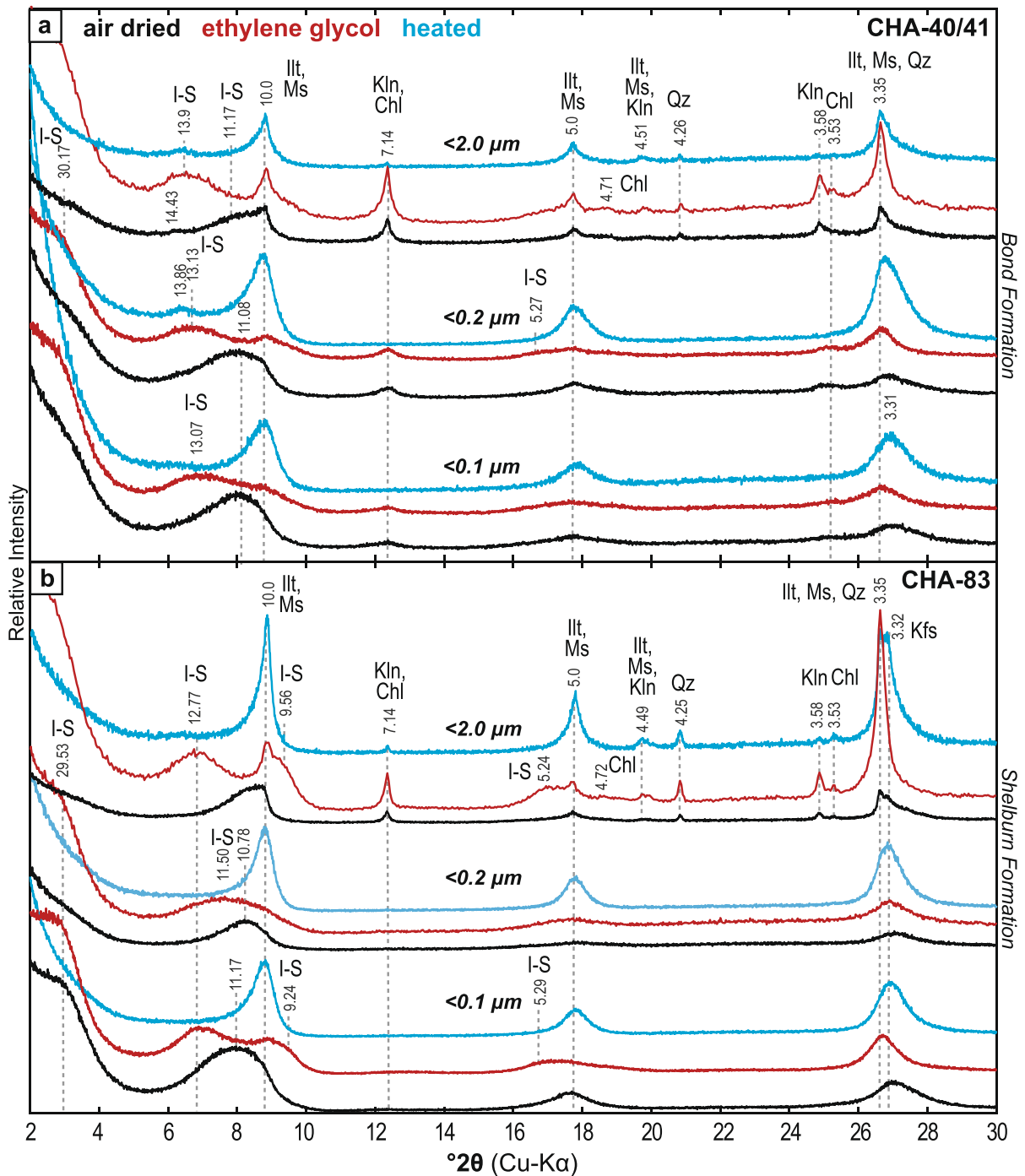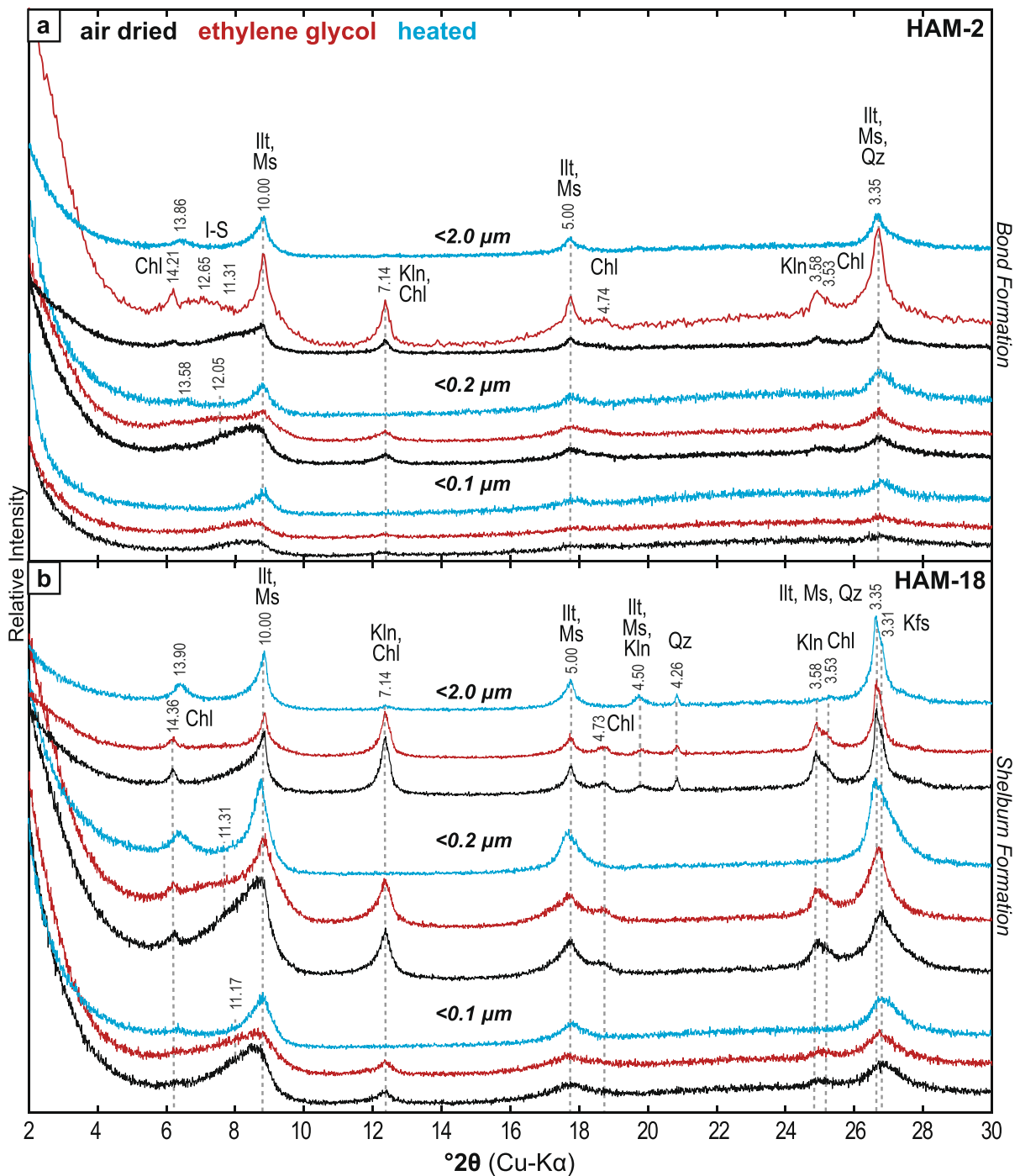
Fig. 4 XRD patterns of oriented aggregates of clay-sized fractions from CHA paleosol matrices. Explanations as in Fig. 3

2.49 Å may correspond to kaolinite, though these are rare to non-existent as they are expected to have collapsed following heating.

I-S and discrete illite or muscovite were the predominant phyllosilicate minerals in most size fractions of all the samples (Table 2). The stacking orders of I-S

Fig. 5 XRD patterns of oriented aggregates of clay-sized fractions from HAM paleosol matrices. Explanations as in Fig. 3

revealed by XRD analyses of ethylene glycol-solvated oriented aggregates were R0, R1, or R3. Three of 18 size fractions contained I-S with R0 and 12 contained

I-S with R1 stacking orders (Figs 3, 4, and 5; Table 2). I-S with R0 occurred only in the northernmost LSC core, in the shallowest sample LSC-16. I-S with R3
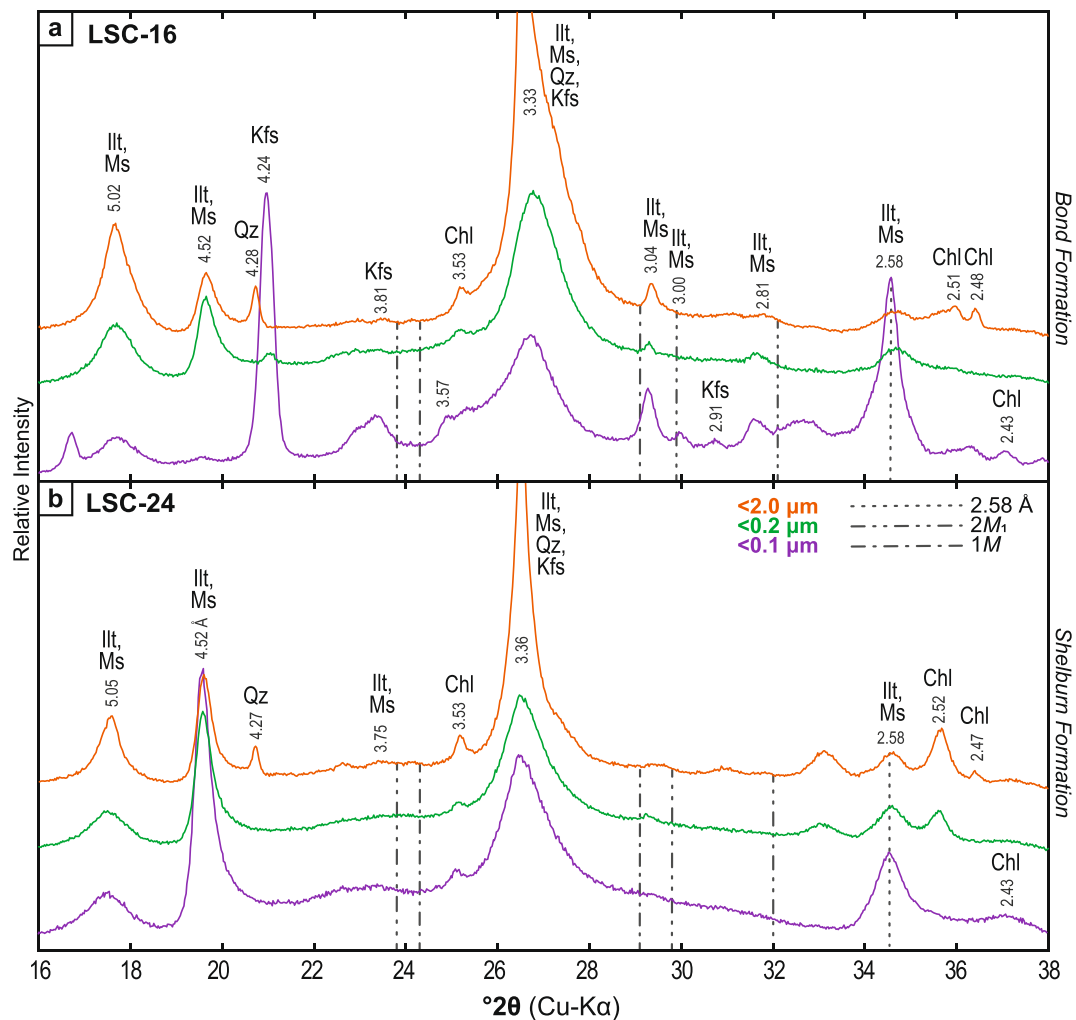
Fig. 6 Stacked XRD patterns of standard powder mounts for illite and mica polytype characterization in the LSC core, that have been heated to 550°C. Interplanar spacings, d_{hkl} (Å) are noted vertically. Light gray dash-dot-dot lines and dash-dot lines denote where $2M_1$ and M_1 illite polytype peaks should be, respectively. Abbreviations of minerals are noted near d values

was the observed stacking order in all clay subfractions of HAM-18 (Table 2).

The mica polytypes were identified by comparing the observed diffraction peaks to the diffraction peaks associated with specific mica polytypes (Figs 6, 7 and 8). The $1M$ and $2M_1$ mica polytype information was not collected from every size fraction of each sample due to lack of significant peaks at the expected positions corresponding to the specific mica polytypes (Figs 6, 7 and 8). Of 18 XRD patterns, five contained peaks associated with the $2M_1$ polytype. The amount of $2M_1$ polytype, calculated from the areas of the 3.00 Å peak and the 2.58 Å

band for those five patterns, varied from 4 to 72% relative to the total amount of all polytypes (Figs 6, 7 and 8; Table 3). There were trace amounts of the $2M_1$ polytype in CHA-40/41 <0.1 μm and HAM-18 <0.2 μm (Table 3). As the areas of the $2M_1$ polytype peaks are very small, the accuracy of those quantitative values is questionable. Small peaks may be due to partial dehydroxylation during preheating of the sample prior to XRD analysis of the size fractions of the standard powder mount. Nevertheless, the existence of $2M_1$ polytype peaks in the clay-sized fractions still has interpretative value and will be discussed simply as an occurrence, not
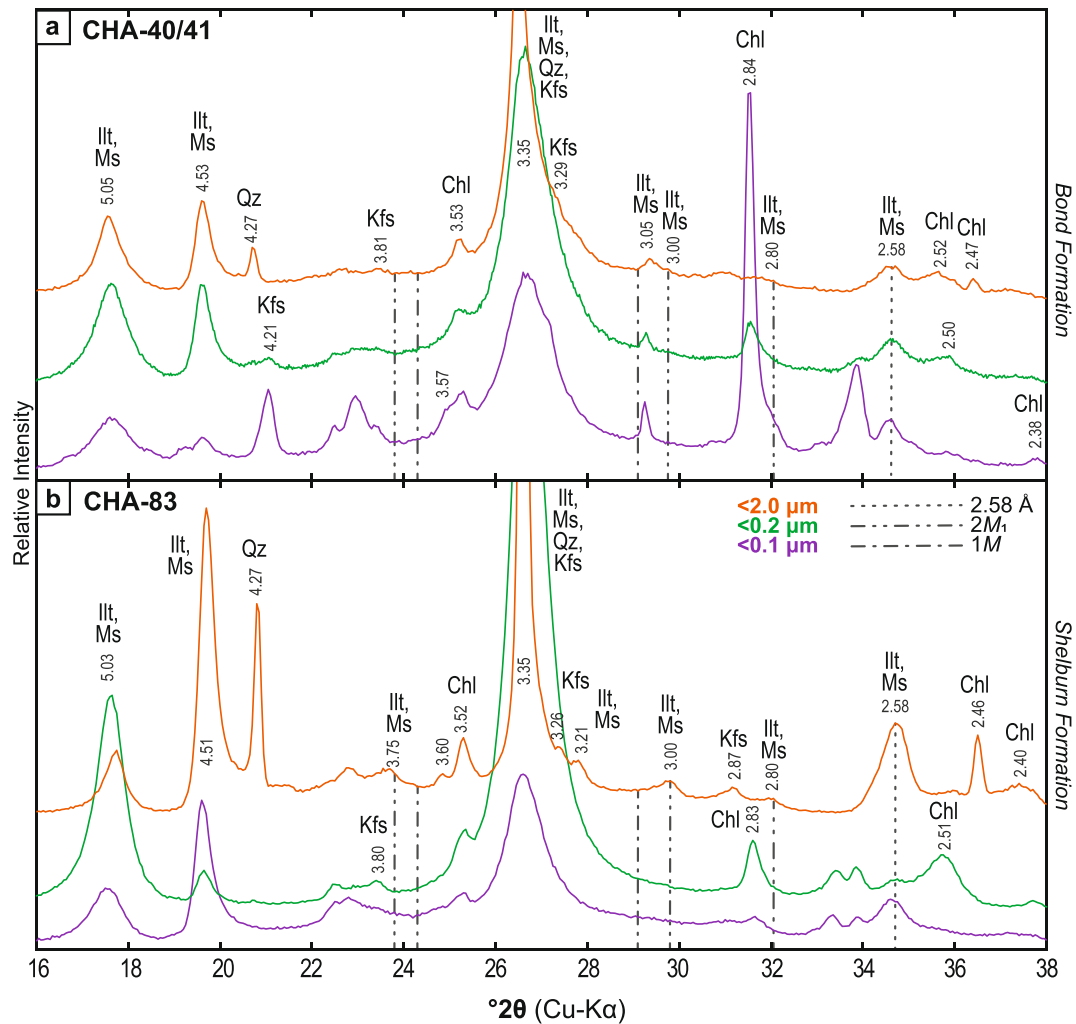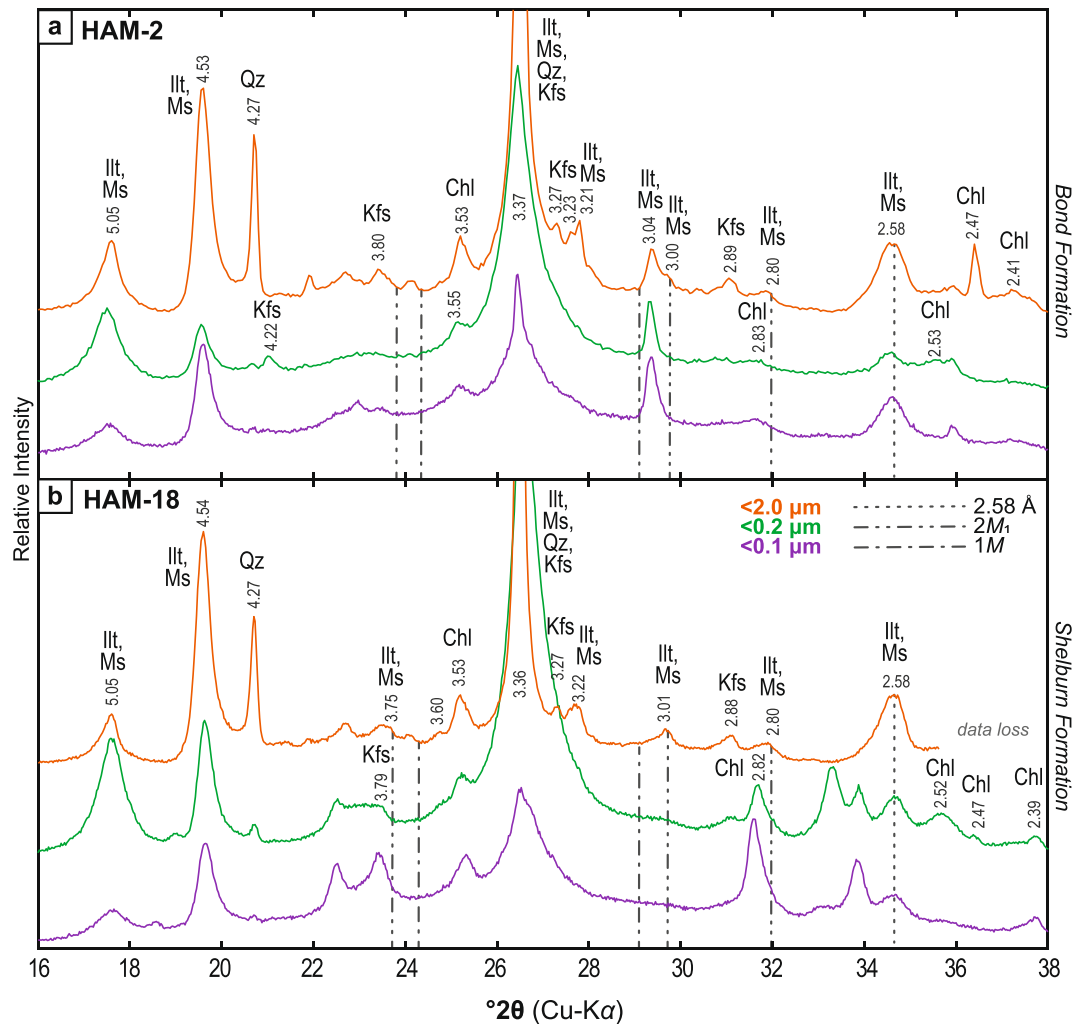
Fig. 7 Stacked XRD patterns of standard powder mounts for illite and mica polytype characterization in the CHA core. Explanations as in Fig. 6

relative abundance, hereafter. None of the XRD patterns showed a peak associated with the 1M polytype (Figs 6, 7 and 8). The remaining mica (not tabulated) belongs to the $1M_d$ polytype (*sensu* Grathoff & Moore (1996); Pevear (1999)). These data indicate that the $1M_d$ polytype is the most common polytype in the studied clay-size fractions of these paleosols.

The polytype analyses of these illitic clays were probably of poor accuracy and, thus, are not definitive for understanding the genetic origins of assemblages of illitic minerals in these paleosols. This is because most of the illitic minerals here are I-S and not discrete and overlap with other minerals in key reflection

positions (Figs 3, 4, and 5; Table 2). Because polytype analyses are typically determined for discrete and not interstratified clay mineral phases, most of these paleosol samples are probably not good candidates for mica-polytype analysis. Future analyses by other methods, such as transmission electron microscopy, may provide more information on the existence and structure of mica polytypes.

The d_{001} reflection of chlorite was best seen in the heat-treated patterns, as interference from I-S was reduced (Figs 3, 4, and 5). Chlorite maintains a small peak width and is most common in the HAM core (Fig. 5). Kaolinite was identified based on the collapse of the d_{001} peak after heating and occurred in most

Fig. 8 Stacked XRD patterns of standard powder mounts for illite and mica polytype characterization in the HAM core. Explanations as in Fig. 6

samples, except the CHA-83 <0.2 µm and <0.1 µm (Figs 3, 4, and 5; blue XRD pattern). Finer size fractions tend to have smaller or absent peaks corresponding to quartz, kaolinite, and chlorite (Figs 3, 4, 5, 6, 7 and 8). Because chlorite, kaolinite, and quartz do not possess K, they did not impact the K-Ar results.

K-feldspars have been identified in non-clay-size fractions of IB paleosols (e.g. Grim & Allen, 1938; Schultz, 1958). XRD *d* values for orthoclase, sanidine, and microcline have intense peaks at ~4.22, 3.77, 3.31, 3.26 Å (Brown, 1980). The XRD patterns presented here of standard powder mount clay-sized fractions (Figs 6, 7 and 8) revealed some minor peaks in positions for those feldspar minerals.

In all cases, e.g. CHA-83 (Fig. 7b), these K-feldspar peaks were more prominent in the <2.0 µm fraction and smaller or absent in the finer fractions (Table 2). This indicates that though finer clay-sized fractions may have some authigenic K-feldspar phases, their K-Ar age values reflect a greater influence by authigenic K-bearing mica minerals.

K-Ar Geochronologic Data

The concentration of potassium varied among the 18 clay-size fractions from 2.73 to 4.79 wt.% K. The K-Ar age values vary from 311 to 218 Ma (Table 4, Fig. 9). Generally, finer fractions have smaller age

Table 2 Minerals in IB paleosols

Sample ID	Clay-sized fraction (μm)	Minerals identified [a]
LSC-16	<2.0	I-S (R0)[b], Mca, Kln, Chl, Qz
	<0.2	I-S (R0), Mca, Kln, Chl
	<0.1	I-S (R0), Mca, Kln, Chl (trace)
LSC-24	<2.0	I-S (R1), Mca, Kln, Chl (trace), Qz
	<0.2	I-S (R1), Mca, Kln, Chl
	<0.1	I-S (R1), Mca, Kln, Chl
CHA-40/41	<2.0	I-S (R1), Mca, Kln, Chl (trace), Qz
	<0.2	I-S (R1), Mca, Kln, Chl (trace)
	<0.1	I-S (R1), Mca, Kln, Chl (trace)
CHA-83	<2.0	I-S (R1), Mca, Kln, Chl (trace), Qz, Kfs
	<0.2	I-S (R1), Mca, Chl (trace)
	<0.1	I-S (R1), Mca, Chl (trace)
HAM-2	<2.0	I-S (R1), Mca, Kln, Chl, Qz
	<0.2	I-S (R1), Mca, Kln, Chl (trace), Qz
	<0.1	I-S (R1), Mca, Kln, Chl (trace)
HAM-18	<2.0	I-S (R3), Mca, Kln, Chl, Qz, Kfs
	<0.2	I-S (R3), Mca, Kln, Chl, Qz, Kfs
	<0.1	I-S (R3), Mca, Kln, Chl (trace), Qz

[a] Minerals identified from XRD analyses of oriented aggregates. I-S = interstratified illite-smectite, Mca = mica group (muscovite or illite), Kln = kaolinite, Chl = chlorite, Qz = quartz, Kfs = K-feldspar group

[b] Stacking order of I-S. R0: random interstratification, R1: short-range ordered, and R3: long-range ordered

values than the coarser fractions of the same samples. In most cases, the age value for the <0.1 μm fraction is less by ~50 million years than that for the <2.0 μm fraction. No overall correlation was found between the age values for a paleosol and its sampling depth (Tables 1, 4). Moreover, age values for specific size fractions from the southernmost core, HAM, were generally larger than those for corresponding

fractions from the central CHA core and northernmost LSC core.

The uncertainties of the K-Ar apparent ages were calculated for the 95% confidence level, or 2σ, and varied from ±5 to ±45 Ma (Table 4). The larger error values, specifically those above ±10 Ma, were due to intermittent failure of the electron-current controller of the ion source of the mass spectrometer during measurement of argon from the first three of the 20 test portions originally prepared for this study. During some of the isotopic analyses after that controller failed, abrupt and relatively large changes occurred in the electron current which caused the ion currents to be inconsistent, leading to irremediable, large variability in calculated isotope ratios. New age values from later, much more precise duplicate analyses were obtained for two of the three fractions for which the original analyses were highly imprecise, but not for the HAM-18 <0.2 μm fraction (Table 4).

A special case is the age value for the <0.1 μm size fraction of sample HAM-2. The mass of that fraction was the smallest of those used for the present K-Ar work, so an attempt was made to dilute its argon with a reduced amount of ^{38}Ar. The result was an age value (of ~450 Ma) inconsistent with the clear pattern of K-Ar age values exhibited by all the other clay-size fractions of the present study. The inconsistency was attributed to an unexplained loss of some of the ^{38}Ar tracer, owing perhaps to a valve not fully closed. Because the amount of ^{38}Ar lost is unknown, the ^{40}Ar content and age value for the HAM-2 <0.1 um fraction was obtained by treating its isotopic analysis as an 'unspiked run,' disregarding the ^{38}Ar signal and assuming that the operational sensitivity for the two other Ar isotopes was the same as in the immediately preceding isotopic analysis. The K-Ar age value obtained in

Table 3 Results of polytype calculations

Sample ID	Clay-sized fraction (μm)	Area of 2.58 Å peak band (2.55–2.59 Å)	Area of 3.74 Å peak	Area of 3.00 Å peak	Area of 2.80 Å peak	$2M_1$ polytype abundance from 3.00 Å peak area (%)
LSC-16	<0.1	97851		5657		20%
CHA-40/41	<2.0	8466		21		5%
	<0.1		trace			
CHA-83	<2.0	39617	4794	4592	5332	40%
HAM-2	<2.0	23301		1123	956	20%
HAM-18	<2.0	45682	7876	9338		70%
	<0.2		trace			

🙋 Springer

Table 4 K-Ar results for clay-sized fractions in IB paleosols

Sample ID	Clay-sized fraction (µm)	K (wt. %)	[40]Ar* (%) [a]	[40]Ar* (nmol/kg)	K-Ar age value (Ma)	K-Ar age value error (± Ma) [b]
LSC-16	<2.0	2.74	89	1378	269	5
	<0.2	3.08	87	1466	256	10
		3.08	91	1464	255	35[c]
	<0.1	2.73	81	1096	218	10
LSC-24	<2.0	3.77	91	1985	281	5
	<0.2	3.94	94	2066	280	10
		3.73	91	1773	255	5
	<0.1	3.98	92	1988	268	10
CHA-40/41	<2.0	3.48	90	1813	278	10
		3.44	82	1767	275	5
		3.46	86	1786	276	5
	<0.2	3.80	92	1894	267	10
	<0.1	3.80	90	1627	231	10
CHA-83	<2.0	3.83	92	2135	296	10
	<0.2	4.79	93	2376	266	10
	<0.1	4.62	95	2596	298	45[c]
		4.62	93	2162	251	10
HAM-2	<2.0	3.59	94	2116	311	35[c]
		3.52	96	1974	297	5
	<0.2	4.25	92	2327	291	15
	<0.1	4.13	78	1827	240[d]	
HAM-18	<2.0	3.80	94	2237	311	10
	<0.2	4.16	94	2401	305	35[c]
	<0.1	4.21	91	2090	266	10

[a] [40]Ar* = radiogenic argon. Remaining percentage is atmospheric [40]Ar

[b] Uncertainties in apparent ages were calculated from the effect of analytical errors at the 95% confidence level (2σ)

[c] During argon-isotope analysis, uncontrolled large changes in electron emission by the mass spectrometer's filament caused unusually large variability in the measured isotope ratios in this case

[d] The uncertainty of this age value is unknown. See text

this way was 240 Ma, which is smaller than those for all other fine fractions for the HAM paleosols, but no value has been estimated for its uncertainty (Table 4). Detailed support for the chosen treatment of this special case is available as Supplementary Information 2.

Discussion

Diagenetic Components of IB Paleosols

K-Ar age values of clay-sized material from middle and upper Pennsylvanian paleosols in this study range from 311 Ma to 218 Ma (Table 3; Fig. 9). Without

other information, the K-Ar age values with error considered (but disregarding that an actual age value could be outside the 95% confidence interval of the analytical result) show that there is diagenetic K-bearing material in all LSC and CHA sample fractions and the finest HAM-18 fraction.

The K-Ar age values presented here showed that paleosol samples contain some diagenetic K-bearing material that formed after the ~270 Ma magmatism in the IKFD (e.g. Reynolds et al., 1997) and during the onset of estimated maximum burial of the IB (e.g. Rowan et al., 2002). These results contrast the findings of the stable isotope study of the same phyllosilicates from IB paleosols by Rosenau and Tabor
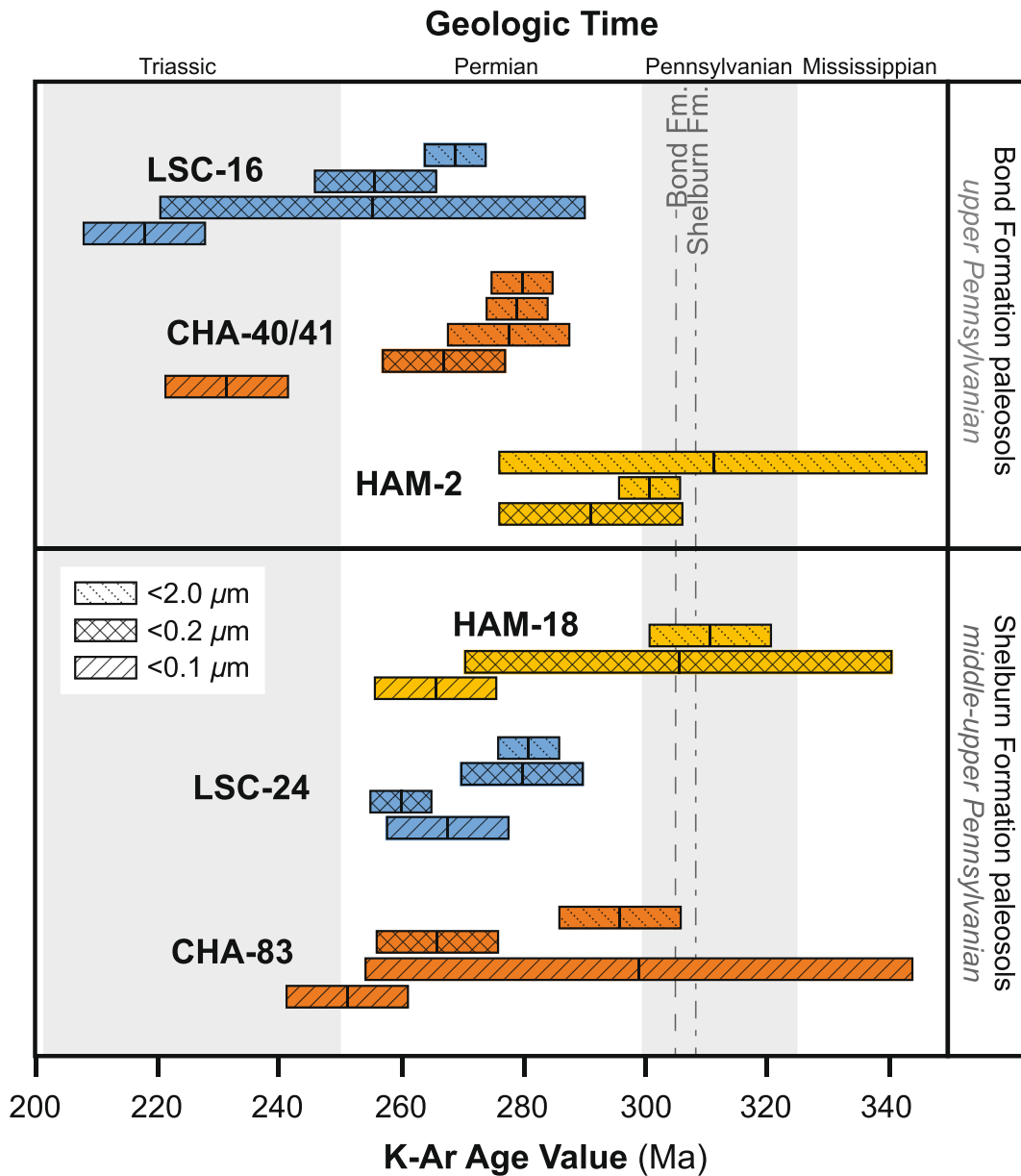
Fig. 9 K-Ar age values from clay-sized fractions of Illinois Basin paleosols on a background depicting the corresponding time periods and the chronostratigraphic positions of the paleosols. Horizontal bars show the ranges of 2σ error associated with the age values

(2013) analyzed in this study. LSC-16 and LSC-24 of mature, calcic Vertisols (Table 1) yielded phyllosilicate crystallization temperatures of 33 and 39°C ± 3°C, respectively, suggesting that the LSC core was mostly void of diagenetic overprinting (Rosenau & Tabor, 2013). Though they attributed LSC trends to a small maximum depth of burial (<1 km) and being distal from any heat sources in the IKFD, they tentatively suggested that LSC-24 temperature is high and may not represent an ancient soil temperature. Despite the occurrence of R0 stacking orders found herein and by Rosenau et al. (2013a) for LSC-16, K-Ar age values from these samples are some of the lowest from all the cores (Fig. 9; Table 4). Thus, K-Ar ages of the LSC core highlight that paleosol morphology, the stacking order of I-S, and the reconstructed

burial depth are not indicative of preservation of original pedogenic minerals or of diagenetic overprinting.

Increased temperatures, high water:rock ratios, abundant aqueous K, and time required to trigger illitization during burial in the IB may have been achieved after the Pennsylvanian. Using a series of numerical models, Rowan et al. (2002) found that combined burial and hydrothermal fluids are both necessary to cause the high coal maturities throughout the IB, though hydrothermal temperatures were probably lower in the north (Fig. 10). Similarly, Mariño et al. (2015) found that the units in the south and central IB near the sub-Absaroka unconformity (Mississippian–Pennsylvanian boundary) and the cleat system of coals may support fluid migration, where the latter is supported by studies of fluid inclusions of minerals in some coals (Cobb, 1981; Whelan et al., 1988). Also, Mariño et al. (2015) suggested that faults in southern regions of the IB that extend from the Precambrian basement into the Paleozoic sediments may provide vertical conduits for fluid flow, albeit only regionally. The findings of these models suggests that heat flow at low temperatures (~100±30°C), if sustained over enough time, may be adequate and available to trigger mineral alteration in Paleozoic formations of the IB in the south and central IB. Yet, it is unclear how these hydrothermal fluids may have migrated vertically and horizontally across the entire IB to geochemically alter the shallow Pennsylvanian paleosols. Particularly for the northernmost LSC core samples, whose maximum burial depth was ~800 m and spatial distance was ~500 km north from the suspected heat source in the IKFD (Figs 1, 9).

Support for low-temperature, time-dependent, or protracted diagenesis to drive illitization processes (*sensu* Velde & Vasseur, 1992) has also been suggested to explain diagenetic illitization in the Devonian-Mississippian New Albany Shale (Gharrabi & Velde, 1995) and the Pennsylvanian Browning Sandstone and Purington Shale (Moore, 2000, 2003). The K-Ar age-value evidence for diagenetic minerals in Pennsylvanian paleosols provides further evidence for protracted diagenesis. This is because K-Ar age values of fine clay-size fractions presented in this study are <270 Ma, but non-equal. The low K-Ar age values of the finest fractions indicate that such illitization would have proceeded most slowly in the LSC-16 paleosol, which is consistent with it having the smallest K content, I-S with R0 stacking order, and being the shallowest sample from the northernmost location. The larger K-Ar age values from the paleosols of the CHA and finest fraction of the HAM cores indicate that illitization may have proceeded more rapidly or ceased earlier than in the LSC core. It should be noted that K-Ar age values cannot resolve whether illitization occurred during one or multiple event(s) (Środoń et al., 2009).
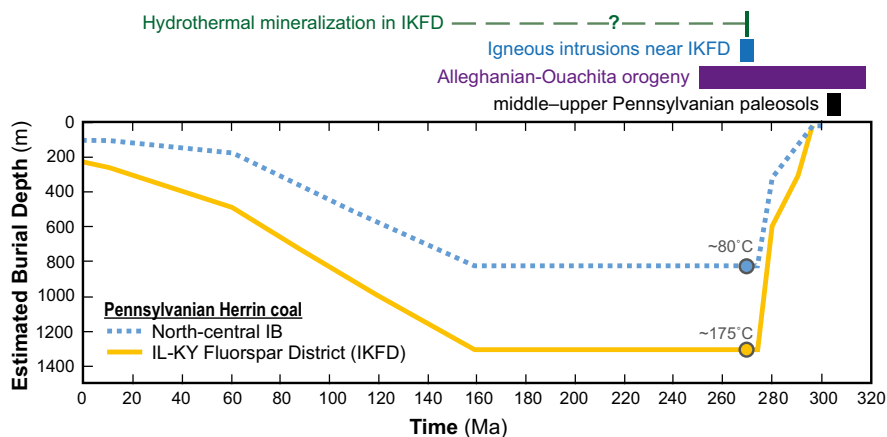
Fig. 10 Estimated burial curves for the Herrin Coal (middle Pennsylvanian, Carbondale Formation; Fig. 2) from the hybrid burial plus hydrothermal fluid flow model of Rowan et al. (2002). Burial curves are coded to locations in the basin (Fig. 1), including the southern Illinois-Kentucky Fluorspar district and a north-central IB location near the Lone Star Cement Company #TH-1 (LSC) core. The modeled temperature of the Herrin Coal at 270 Ma is ~80°C in the north central IB and ~175°C in the Illinois Kentucky Fluorspar district

Detrital Components of IB Paleosols

K-Ar age values alone cannot diagnose the presence of either detrital or pedogenic K-bearing material in any of the clay fractions studied. Yet, K-Ar age values do not rule out the presence of either detrital or pedogenic K-bearing material in any of the clay fractions studied.

K-Ar age values are generally largest in size fractions from the HAM core in the southern IB and smallest in the northern LSC core (Figs 1, 9). This may indicate that the HAM core has more detrital minerals in the clay-sized fractions than the other cores. HAM-18 was from a paleosol that was classified as a gleyed Protosol (Table 1), which means that it is an immature paleosol with some gleyed properties such as grey matrix color (G14-15/N; Munsell Color, 1975), sulfide mineralization, and other redoximorphic features (McIntosh, 2018). The HAM-18 sample possesses more of the $2M_1$ polytype (relative to all micas) than all the other samples (Fig. 8; Table 3). This mineral is probably muscovite rather than an illite, which is supported by the presence of the sharp and tall 10 Å peaks from XRD of oriented aggregates from the HAM core (Fig. 5). Particularly in the patterns of heated HAM-18 clay-size fractions (Fig. 5b) in which smectitic interlayers would have collapsed due to dehydration, these 10 Å peaks are sharper than in XRD patterns of oriented aggregates that were air dried and glycolated. The immaturity indicated by the morphology of the HAM-18 Protosol is consistent with its coarsest fraction probably having an actual age value greater than that of any other studied fraction, because less smectite would have been available therein for illitization during diagenesis.

Conversely, all the other paleosols sampled from the central CHA and northern LSC cores for this work are more mature paleosols identified as Vertisols, with calcic and gleyed features. The LSC core contains the only I-S with R0 stacking order, of sample LSC-16 (Fig. 3; Table 2), while LSC-24 and both CHA samples exhibit I-S with R1 stacking order, except for CHA-83 <0.2 μm which has I-S with R3 (Fig. 3, Table 2). Moreover, the clay-size fractions from the more morphologically developed paleosols (e.g. CHA) have a greater relative abundance of $1M_d$ illite polytypes than does HAM-18 <2.0 μm (Table 3).

The greater presence of quartz in <2.0 μm clay-size fractions, notable by the *d* value at ~4.26 Å, which decreases or is absent from finer clay-size fractions of all paleosol samples supports the notion that there are more detectable detrital minerals in larger clay-size fractions. The additional presence of both $2M_1$ mica and K-feldspar in HAM and CHA <2.0 μm suggests that these minerals are detrital. The presence of more detrital material in these fractions than in all other fractions studied is consistent with K-Ar age values for three out of four of these <2.0 μm fractions being considerably greater than in nearly all finer fractions. Previous studies of IB paleosols found evidence for potassic feldspars in non-clay-size fractions, finding no clear vertical variation in K-feldspar abundances within a particular paleosol profile (e.g. Grim & Allen, 1938; Schultz, 1958). Schultz (1958) interpreted this to mean that the K-feldspars have not been weathered significantly since their inheritance, indicating that K-feldspars in these units are mostly detrital and not authigenic.

A greater quantity of detrital minerals in paleosols from the southern and central IB is consistent with the understanding of the burial of the IB and paleosol occurrence. Gharrabi and Velde (1995) suggested that burial of at least 1.5 km began in the Mesozoic and continued into the Paleogene, until erosion began at ~50 Ma. The southern IB had greater accommodation as it was probably buried to depths of ~3 km, while the northern IB was buried to depths of ~1 km (Rowan et al., 2002). Protosols in the IB are probably weakly developed due to formation on an unstable landscape, where there was intermittent and rapid sediment supply. The southern HAM core contains more Protosols than the CHA (see table 1 in McIntosh et al., 2021) or LSC cores (see Pedotype B in table 3 of Rosenau et al., 2013a) in Pennsylvanian strata of the IB. As a result, combined K-Ar age values; mineralogic, petrologic, and basin analysis; and depositional environment considerations provide support for the presence of more detrital minerals in clay-size fractions of IB paleosols from the HAM core in the southern IB, compared to the other more northern, shallowly buried cores.

Conclusions

The mineralogical and geochronometric results of the present study provide robust support for the hypothesis that Pennsylvanian paleosols of the Illinois Basin are not exclusively comprised of pedogenic I-S, but also have both detrital muscovite and diagenetic illitic

minerals. Despite shallow maximum burial depths, this work found that increased abundances of detritus are correlated to increased burial depth, highlighting the importance of understanding a basin's evolution before and after soil and paleosol formation. Because this work cannot precisely resolve how diagenetic illitization conditions were favorable across the entire IB at any particular period in the geological past, and the effects of hydrothermal fluids may only be localized rather than basin-wide, illitization in Illinois Basin paleosols was more likely initiated during protracted diagenesis. This work demonstrates that shallowly buried paleosols and the sedimentary basin in which they form should be characterized extensively before minerals from those paleosols are used to reconstruct ancient climates and environments.

Data Availability   All data generated or analyzed during this study are included in this published article and its supplementary information files.

Declarations

Conflicts of Interest   The authors declare that they have no conflict of interest.

References

Altschaeffl, A. G., & Harrison, P. W. (1959). Estimation of a minimum depth of burial for a Pennsylvanian underclay. *Journal of Sedimentary Research, 29*, 178–185.

Bailey, S. W., Hurley, P. M., Fairbairn, H. W., & Pinson, W. H., Jr. (1962). K-Ar dating of sedimentary illite polytypes. *Geological Society of America Bulletin, 73*, 1167–1170.

Barrows, M. H. (1985). *Occurrence and maturation of sedimentary organic matter in the Illinois Basin [Summary Report]*. Illinois State Geological Survey.

Bechtel, A., Elliott, W. C., Wampler, J. M., & Oszczepalski, S. (1999). Clay mineralogy, crystallinity, and K-Ar ages of illites within the Polish Zechstein Basin; Implications for the age of Kupferschiefer mineralization. *Economic Geology, 94*, 261–272.

Boles, J. R., & Franks, S. G. (1979). Clay diagenesis in Wilcox sandstones of Southwest Texas; Implications of smectite diagenesis on sandstone cementation. *Journal of Sedimentary Research, 49*, 55–70.

Bradbury, J. C., & Baxter, J. W. (1992). *Intrusive breccias at Hicks Dome Hardin County (Circular 550)*. Illinois, Illinois State Geological Survey.

Brannon, J. C., Leach, D. L., Goldhaber, M. G., Taylor, C. D., & Livingstone, E. (1997) Radiometric dating of ore stage calcite from Knight Vein, IL-KT Fluorspar District, yields 195 Ma for both U-Pb and Th-Pb systems. P. A-209 In: *Geological Society of America Abstracts with Programs*.

Brindley, G. W. (1961). Kaolin, serpentine, and kindred minerals. In G. Brown (Ed.), *The X-ray identification and crystal structures of clay minerals* (2nd ed., pp. 51–131). Mineralogical Society.

Brindley, G. W., & Brown, G. (Eds.). (1980). *Crystal structures of clay minerals and their x-ray identification*. Mineralogical Society.

Brown, G. (1980). Associated Minerals. In G. W. Brindley & G. Brown (Eds.), *Crystal Structures of Clay Minerals and their X-ray Identification* (pp. 361–410). Mineralogical Society.

Buschbach, T. C., & Kolata, D. R. (1990). Regional setting of Illinois Basin: Chapter 1: Part I. Illinois Basin: Regional setting. In M. W. Leighton, D. R. Kolata, D. F. Oltz, & J. J. Eidel (Eds.), *Interior Cratonic Basins* (51st ed., pp. 29–55). American Association of Petroleum Geologists.

Cecil, C. B., DiMichele, W. A., & Elrick, S. D. (2014). Middle and Late Pennsylvanian cyclothems, American Midcontinent: Ice-age environmental changes and terrestrial biotic dynamics. *Comptes Rendus Geoscience, 346*, 159–168.

Chesley, J. T., Halliday, A. N., Kyser, T. K., & Spry, P. G. (1994). Direct dating of Mississippi Valley-type mineralization; use of Sm-Nd in fluorite. *Economic Geology, 89*, 1192–1199.

Clauer, N. (2013). The K-Ar and ^{40}Ar/^{39}Ar methods revisited for dating fine-grained K-bearing clay minerals. *Chemical Geology, 354*, 163–185.

Cluff, R. M., & Byrnes, A. P. (1990). Lopatin Analysis of maturation and petroleum generation in the Illinois basin. In M. W. Leighton, D. R. Kolata, D. F. Oltz, & J. J. Eidel (Eds.), *Interior Cratonic Basins* (51st ed., pp. 425–454). American Association of Petroleum Geologists.

Cobb, J. C. (1981) Geology and geochemistry of sphalerite in coal. Ph.D. Dissertation, University of Illinois Champaign-Urbana, Champaign, p 202.

Cohen, K. M., Finney, S. C., Gibbard, P. L., & Fan, J.-X. (2013). The ICS International Chronostratigraphic Chart. *Episodes, 36*, 199–204.

Crowell, J. C., & Frakes, L. A. (1970). Phanerozoic glaciation and the causes of ice ages. *American Journal of Science, 268*, 193–224.

Curtis, C. D. (1985). Clay mineral precipitation and transformation during burial diagenesis. *Philosophical Transactions of the Royal Society of London Series A, Mathematical and Physical Sciences, 315*, 91–105.

Damberger, H. H. (1971). Coalification pattern of the Illinois Basin. *Economic Geology, 66*, 488–494.

Davydov, V. I., Crowley, J. L., Schmitz, M. D., & Poletaev, V. I. (2010) High-precision U-Pb zircon age calibration of the global Carboniferous time scale and Milankovitch band cyclicity in the Donets Basin, Eastern Ukraine. *Geochemistry, Geophysics, Geosystems, 11*(2),1–22. https://doi.org/10.1029/2009GC002736.

De Man, E., Van Simaeys, S., Vandenberghe, N., Harris, W. B., & Wampler, J. M. (2010). On the nature and chronostratigraphic position of the Rupelian and Chattian stratotypes in the southern North Sea basin. *Episodes, 33*, 3–14.

Denny, F. B. (2005) The Cottage Grove dike and mafic igneous intrusions in southeastern Illinois and their relation to regional tectonics and economic resources. M.S. Thesis, Southern Illinois University, Carbondale.

Denny, F. B., Goldstein, A., Devera, J. A., Williams, D. A., Lasemi, Z., & Nelson, W. J. (2008). The Cottage Grove dike and mafic igneous intrusions in southeastern Illinois and their relation to regional tectonics and economic resources [M.Sc. Thesis, Southern Illinois University]. ProQuest Dissertations and Theses Global.

DiMichele, W. A., & Phillips, T. L. (1996). Climate change, plant extinctions and vegetational recovery during the Middle-Late Pennsylvanian Transition: The case of tropical peat-forming environments in North America. *Geological Society, London, Special Publications, 102*, 201–221.

DiMichele, W. A., Tabor, N. J., Chaney, D. S., & Nelson, W. J. (2006) From wetlands to wet spots: Environmental tracking and the fate of Carboniferous elements in Early Permian tropical floras. In S. F. Greb & W. A. DiMichele (Eds.), *Wetlands through Time* (Vol. 399). Geological Society of America.

Domeier, M., Van der Voo, R., & Torsvik, T. H. (2012). Paleomagnetism and Pangea: The road to reconciliation. *Tectonophysics, 514–517*, 14–43.

Dong, H., Jaisi, D. P., Kim, J., & Zhang, G. (2009). Microbe-clay mineral interactions. *American Mineralogist, 94*, 1505–1519.

Eberl, D. D. (1984). Clay mineral formation and transformation in rocks and soils. *Philosophical Transactions of the Royal Society of London Series A, Mathematical and Physical Sciences, 311*, 241–257.

Eberl, D. D., Środoń, J., & Northrop, H. R. (1987). Potassium fixation in smectite by wetting and drying. In J. A. Davis & K. F. Hayes (Eds.), *Geochemical Processes at Mineral Surfaces* (Vol. 323, pp. 296–326). American Chemical Society. https://doi.org/10.1021/bk-1987-0323.ch014

Elliott, W. C., Basu, A., Wampler, J. M., Elmore, R. D., & Grathoff, G. H. (2006). Comparison of K-Ar ages of diagenetic illite-smectite to the age of a chemical remanent magnetization (CRM): An example from the Isle of Skye, Scotland. *Clays and Clay Minerals, 54*, 314–323.

Elsass, F., Środoń, J., & Robert, M. (1997). Illite-smectite alteration and accompanying reactions in a Pennsylvanian underclay studied by TEM. *Clays and Clay Minerals, 45*, 390–403.

Engels, J. C., & Ingamells, C. O. (1977). Geostandards – A new approach to their production and use. *Geostandards Newsletter, 1*, 51–60.

Eslinger, E., Highsmith, P., Albers, D., & deMayo, B. (1979). Role of iron reduction in the conversion of smectite to illite in bentonites in the disturbed belt, Montana. *Clays and Clay Minerals, 27*(5), 327–338.

Fielding, C. R. (2021). Late Palaeozoic cyclothems – A review of their stratigraphy and sedimentology. *Earth-Science Reviews, 217*, 103612.

Fifarek, R. H., Denny, F. B., Snee, L. W., & Miggins, D. P. (2001) Permian igneous activity in southeastern Illinois and western Kentucky: Implications for tectonism and economic resources. P. A-420 In: *Geological Society of America, Abstracts with Programs*.

Gharrabi, M., & Velde, B. (1995). Clay mineral evolution in the Illinois Basin and its causes. *Clay Minerals, 30*, 353–364.

Grathoff, G. H., & Moore, D. M. (1996). Illite polytype quantification using WILDFIRE© calculated X-ray diffraction patterns. *Clays and Clay Minerals, 44*, 835–842.

Grathoff, G. H., Moore, D. M., Hay, R. L., & Wemmer, K. (2001). Origin of illite in the lower Paleozoic of the Illinois basin: Evidence for brine migrations. *GSA Bulletin, 113*, 1092–1104.

Grim, R. E., & Allen, V. T. (1938). Petrology of the Pennsylvanian underclays of Illinois. *GSA Bulletin, 49*, 1485–1514.

Grim, R. E., Bray, R. H., & Bradley, W. F. (1937). The mica in argillaceous sediments. *American Mineralogist, 22*, 813–829.

Guggenheim, S., Adams, J. M., Bain, D. C., Bergaya, F., Brigatti, M. F., Drits, V. A., Formoso, M. L. L., Galán, E., Kogure, T., & Stanjek, H. (2006). Summary of recommendations of nomenclature committees relevant to clay mineralogy: Report of the Association Internationale Pour L'etude Des Argiles (AIPEA) Nomenclature Committee for 2006. *Clays and Clay Minerals, 54*, 761–772.

Guggenheim, S., Adams, J. M., Bain, D. C., Bergaya, F., Brigatti, M. F., Drits, V. A., Formoso, M. L. L., Galán, E., Kogure, T., & Stanjek, H. (2007). Corrigendum 1 Summary of recommendations of Nomenclature Committees Relevant to Clay Mineralogy: Report of the Association Internationale pour l'Etude des Argiles (AIPEA) Nomenclature Committee for 2006. *Clay Minerals* (42nd ed., pp. 575–577). Cambridge University Press.

Heckel, P. H. (1994). Evaluation of evidence for glacio-eustatic control over marine Pennsylvanian cyclothems in North

America and consideration of possible tectonic effects. *Tectonic and Eustatic Controls on Sedimentary Cycles, 4*, 65–87.

Heckel, P. H. (2008). Pennsylvanian cyclothems in Midcontinent North America as far-field effects of waxing and waning of Gondwana ice sheets. *Geological Society of America Special Papers, 441*, 275–289.

Hower, J. C. (1981). X-ray diffraction identification of mixed-layer clay minerals. In F. J. Longstaffe (Ed.), *Short Course in Clays and the Resource Geologist* (Vol. 7, pp. 39–59). Mineralogical Society of Canada.

Hower, J., Eslinger, E. V., Hower, M. E., & Perry, E. A. (1976). Mechanism of burial metamorphism of argillaceous sediment: 1. Mineralogical and chemical evidence. *Geological Society of America Bulletin, 87*, 725–737.

Huddle, J. W., & Patterson, S. H. (1961). Origin of Pennsylvanian underclay and related seat rocks. *Geological Society of America Bulletin, 72*, 1643–1660.

Hughes, R. E., De Maris, P. J., White, W. A., & Cowin, D. K. (1985). Origin of Clay Minerals in Pennsylvanian Strata of the Illinois Basin. In L. G. Schultz, H. van Olphen, & F. A. Mumpton (Eds.), *Proceedings of the International Clay Conference, Denver* (pp. 97–104). The Clay Minerals Society.

Hurley, P. M., Cormier, R. F., Hower, J., Fairbairn, H. W., & Pinson, W. H., Jr. (1960). Reliability of glauconite for age measurement by K-Ar and Rb-Sr methods. *AAPG Bulletin, 44*, 1793–1808.

Jackson, M. L. (2005). *Soil chemical analysis advanced course* (2nd ed.). Parallel Press, University of Wisconsin-Madison Libraries.

Jagodzinski, H. (1949). *Eindimensionale Fehlordnung in Kristallen und ihr Einfluss auf die Röntgeninterferenzen. I. Berechnung des Fehlordnungsgrades aus den Röntgenintensitäten* (pp. 201–207). *Acta Crystallographica*. International Union of Crystallography.

Kinter, E. B., & Diamond, S. (1956). A new method for preparation and treatment of oriented-aggregate specimens of soil clays for X-ray diffraction analysis. *Soil Science, 81*, 111–120.

Kissock, J. K., Finzel, E. S., Malone, D. H., & Craddock, J. P. (2018). Lower-Middle Pennsylvanian strata in the North American midcontinent record the interplay between erosional unroofing of the Appalachians and eustatic sea-level rise. *Geosphere, 14*, 141–161.

Kolata, D. R., & Nelson, W. J. (1990a) Tectonic history of the Illinois basin. In M. W. Leighton, D. R. Kolata, D. F. Oltz, & J. J. Eidel (Eds.), *Interior Cratonic Basins* (Vol. 51, pp. 263–285). American Association of Petroleum Geologists.

Kolata, D. R., & Nelson, W. J. (1990). Basin-forming mechanisms of the Illinois Basin. In M. W. Leighton, D. R. Kolata, D. F. Oltz, & J. J. Eidel (Eds.), *Interior cratonic basins* (pp. 287–292). American Association of Petroleum Geologists.

Lander, R. H., Bloch, S., Mehta, S., & Atkinson, C. D. (1991). Burial diagenesis of paleosols in the giant Yacheng Gas Field, People's Republic of China: Bearing on illite reaction pathways. *Journal of Sedimentary Petrology, 61*, 256–268.

Lawton, T. F., Blakey, R. C., Stockli, D. F., & Liu, L. (2021). Late Paleozoic (Late Mississippian-Middle Permian) sediment provenance and dispersal in western equatorial Pangea. *Palaeogeography, Palaeoclimatology, Palaeoecology, 572*, 110386.

Lu, G., Marshak, S., & Kent, D. V. (1990). Characteristics of magnetic carriers responsible for Late Paleozoic remagnetization in carbonate strata of the mid-continent, U.S.A. *Earth and Planetary Science Letters, 99*, 351–361.

Mack, G. H., James, W. C., & Monger, H. C. (1993). Classification of paleosols. *Geological Society of America Bulletin, 105*, 129–136.

Mariño, J., Marshak, S., & Mastalerz, M. (2015). Evidence for stratigraphically controlled paleogeotherms in the Illinois Basin based on vitrinite-reflectance analysis: Implications for interpreting coal-rank anomalies. *AAPG Bulletin, 99*, 1803–1825.

McCarty, D. K., Sakharov, B. A., & Drits, V. A. (2008). Early clay diagenesis in Gulf Coast sediments: New insights from XRD profile modeling. *Clays and Clay Minerals, 56*, 359–379.

McIntosh, J. A. (2018) *An analysis of mixed-layer clay minerals and major element geochemical trends in middle-upper Pennsylvanian-aged paleosols as a proxy for characterizing basin-wide diagenetic patterns and the paleoenvironment of the Illinois Basin, U.S.A.* [Masters Thesis, Southern Methodist University]. ProQuest Dissertations and Theses Global.

McIntosh, J. A., Tabor, N. J., & Rosenau, N. A. (2021). Mixed-layer illite-smectite in Pennsylvanian-aged paleosols: assessing sources of illitization in the Illinois Basin. *Minerals, 11*, 108.

Montañez, I. P. (2022). Current synthesis of the penultimate icehouse and its imprint on the Upper Devonian through Permian stratigraphic record. *Geological Society, London, Special Publications, 512*, 213–245.

Moore, D. M., & Reynolds, R. (1997). *X-Ray Diffraction and the Identification and Analysis of Clay Minerals*. Oxford University Press.

Moore, D. M. (2000). Diagenesis of the Purington Shale in the Illinois Basin and implications for the diagenetic state of sedimentary rocks of shallow Paleozoic basins. *The Journal of Geology, 108*, 553–567.

Moore, D. M. (2003). *Mineralogy and Diagenesis of the Pennsylvanian Browning Sandstone on the Western Shelf of the Illinois Basin (Circular 561)* (p. 13). Illinois State Geological Survey.

Mora, C. I., Sheldon, B. T., Elliott, W. C., & Driese, S. G. (1998). An oxygen isotope study of illite and calcite in three Appalachian Paleozoic vertic Paleosols. *Journal of Sedimentary Research, 68*, 456–464.

Munsell Color. (1975). *Munsell soil color charts*. Munsell Color.

Nesbitt, H. W. (1992). Diagenesis and metasomatism of weathering profile, with emphasis on Precambrian paleosols. In I. P. Martini & W. Chesworth (Eds.), *Weathering, Soils, & Paleosols* (pp. 127–151). Elsevier.

O'Brien, N. R. (1964). Origin of Pennsylvanian Underclays in the Illinois Basin. *GSA Bulletin, 75*, 823–832.

⚫ Springer

Odin, G. S., et al. (1982). Interlaboratory standards for dating purposes. In G. S. Odin (Ed.), *Numerical Dating in Stratigraphy* (1st ed., pp. 123–150). Wiley Interscience.

Parham, W. E. (1963). Lateral clay mineral variations in certain Pennsylvanian underclays. *Clays and Clay Minerals, 12*, 581–602.

Perry, E., & Hower, J. (1970). Burial diagenesis in Gulf Coast pelitic sediments. *Clays and Clay Minerals, 18*, 165–177.

Pevear, D. R. (1999). Illite and hydrocarbon exploration. *Proceedings of the National Academy of Sciences, 96*, 3440–3446.

Phillips, T. L., Peppers, R. A., Avcin, M. J., & Laughnan, P. F. (1974). Fossil plants and coal: patterns of change in Pennsylvanian coal swamps of the Illinois Basin. *Science, 184*, 1367–1369.

Plumlee, G. S., Goldhaber, M. B., & Rowan, E. L. (1995). The potential role of magmatic gases in the genesis of Illinois-Kentucky fluorspar deposits; implications from chemical reaction path modeling. *Economic Geology, 90*, 999–1011.

Potter, P. E. (1963). Late Paleozoic sandstones of the Illinois Basin. *Report of Investigations*. Illinois State Geological Survey.

Potter, P. E., & Glass, H. D. (1958). Petrology and sedimentation of the Pennsylvanian sediments in southern Illinois: a vertical profile. *Illinois State Geological Survey Report of Investigations*. Illinois State Geological Survey.

Potter, P. E., & Pryor, W. A. (1961). Dispersal centers of Paleozoic and later clastics of the upper Mississippi Valley and adjacent areas. *Geological Society of America Bulletin, 72*, 1195.

Retallack, G. J. (1988). Field recognition of paleosols. In J. Reinhardt & W. R. Sigleo (Eds.), *Paleosols and Weathering through Geologic Time Principles and Applications* (216th ed., pp. 1–20). Geological Society of America.

Reynolds, R. C. (1980). Interstratified clay minerals. In G. W. Brindley & G. Brown (Eds.), *Crystal Structures of Clay Minerals and their X-Ray Identification* (pp. 249–303). Mineralogical Society of Great Britain and Ireland. https://doi.org/10.1180/mono-5.4

Reynolds, R. L., Goldhaber, M. B., & Snee, L. W. (1997) *Paleomagnetic and $^{40}Ar/^{39}Ar$ results from the grant intrusive Breccia and comparison to the Permian Downeys Bluff Sill–Evidence for Permian igneous activity at hicks dome, Southern Illinois Basin* (U.S. Geological Survey Bulletin 2094–G, p. 16). U.S. Geological Survey. https://doi.org/10.3133/b2094G

Rieder, M., Cavazzini, G., D'yakonov, Y. S., Frank-Kamenetskii, V. A., Gottardi, G., Guggenheim, S., Koval', P. W., Müller, G., Neiva, A. M. R., Radoslovich, E. W., Robert, J.-L., Sassi, F. P., Takeda, H., Weiss, Z., & Wones, D. R. (1998). Nomenclature of the Micas. *Clays and Clay Minerals, 46*, 586–595.

Rimmer, S., & Eberl, D. D. (1982). Origin of an underclay as revealed by vertical variations in mineralogy and chemistry. *Clays and Clay Minerals, 30*, 422–430.

Rosenau, N. A., & Tabor, N. J. (2013). Oxygen and hydrogen isotope compositions of paleosol phyllosilicates: Differential burial histories and determination of Middle-Late Pennsylvanian low-latitude terrestrial paleotemperatures. *Palaeogeography, Palaeoclimatology, Palaeoecology, 392*, 382–397.

Rosenau, N. A., Tabor, N. J., Elrick, S. D., & Nelson, W. J. (2013). Polygenetic history of paleosols in middle–upper Pennsylvanian cyclothems of the Illinois Basin, U.S.A.: Part I. characterization of paleosol types and interpretation of pedogenic processes. *Journal of Sedimentary Research, 83*, 606–636.

Rosenau, N. A., Tabor, N. J., Elrick, S. D., & Nelson, W. J. (2013). Polygenetic history of paleosols in middle–upper Pennsylvanian cyclothems of the Illinois Basin, U.S.A.: Part II. integrating geomorphology, climate, and glacioeustasy. *Journal of Sedimentary Research, 83*, 637–668.

Rowan, E. L., & de Marsily, G. (2001). Infiltration of Late Palaeozoic evaporative brines in the Reelfoot rift: a possible salt source for Illinois basin formation waters and MVT mineralizing fluids. *Petroleum Geoscience, 7*, 269–279.

Rowan, E. L., Goldhaber, M. B., & Hatch, J. R. (2002). Regional fluid flow as a factor in the thermal history of the Illinois Basin: Constraints from fluid inclusions and the maturity of Pennsylvanian coals. *AAPG Bulletin, 86*, 257–277.

Ruiz, J., Richardson, C. K., & Patchett, P. J. (1988). Strontium isotope geochemistry of fluorite, calcite, and barite of the Cave-in-Rock fluorite district, Illinois. *Economic Geology, 83*, 203–210.

Savin, S. M., & Hsieh, J. C. C. (1998). The hydrogen and oxygen isotope geochemistry of pedogenic clay minerals: principles and theoretical background. *Geoderma, 82*, 227–253.

Schimmelmann, A., Mastalerz, M., Gao, L., Sauer, P. E., & Topalov, K. (2009). Dike intrusions into bituminous coal, Illinois Basin: H, C, N, O isotopic responses to rapid and brief heating. *Geochimica et Cosmochimica Acta, 73*, 6264–6281.

Schmitz, M. D., & Davydov, V. I. (2012). Quantitative radiometric and biostratigraphic calibration of the Pennsylvanian-Early Permian (Cisuralian) time scale and pan-Euramerican chronostratigraphic correlation. *GSA Bulletin, 124*, 549–577.

Schultz, L. G. (1958). Petrology of underclays. *GSA Bulletin, 69*, 363–402.

Sheldon, N. D., & Tabor, N. J. (2009). Quantitative paleoenvironmental and paleoclimatic reconstruction using paleosols. *Earth-Science Reviews, 95*, 1–52.

Shen, S., & Stucki, J. W. (1994). Effects of Iron Oxidation State on the Fate and Behavior of Potassium in Soils. In J. L. Havlin, J. S. Jacobsen, D. F. Leikam, P. E. Fixen, & G. W. Hergert (Eds.), *Soil Testing: Prospects for Improving Nutrient Recommendations* (40th ed., pp. 173–185). Soil Science Society of America.

Sheppard, S. M. F., & Gilg, H. A. (1996). Stable isotope geochemistry of clay minerals. *Clay Minerals, 31*, 1–24.

Snee, L. W., & Hays, T. S. (1992). $^{40}Ar/^{39}Ar$ geochronology of intrusive rocks and Mississippi-Valley-type mineralization and alteration from the Illinois-Kentucky Fluorspar district. In M. B. Goldhaber & J. J. Eidel (Eds.), *Mineral Resources of the Illinois Basin in the Context of Basin Evolution* (pp. 59–60). U.S. Geological Survey.

Środoń, J. (1999). Extracting K-Ar ages from shales: a theoretical test. *Clay Minerals, 34*, 375–378.

Środoń, J. (1999). Nature of Mixed-Layer Clays and Mechanisms of Their Formation and Alteration. *Annual Review of Earth and Planetary Sciences, 27*, 19–53.

Ⓐ Springer

Środoń, J., Clauer, N., & Eberl, D. D. (2002). Interpretation of K-Ar dates of illitic clays from sedimentary rocks aided by modeling. *American Mineralogist, 87*, 1528–1535.

Środoń, J., Clauer, N., Huff, W., Dudek, T., & Banaś, M. (2009). K-Ar dating of the Lower Palaeozoic K-bentonites from the Baltic Basin and the Baltic Shield: implications for the role of temperature and time in the illitization of smectite. *Clay Minerals, 44*, 361–387.

Steiger, R. H., & Jäger, E. (1977). Subcommission on geochronology: Convention on the use of decay constants in geo- and cosmochronology. *Earth and Planetary Science Letters, 36*, 359–362.

Symons, D. T. A. (1994). Paleomagnetism and the Late Jurassic genesis of the Illinois-Kentucky fluorspar deposits. *Economic Geology, 89*, 438–449.

Tabor, N. J., & Myers, T. S. (2015). Paleosols as indicators of paleoenvironment and paleoclimate. *Annual Review of Earth and Planetary Sciences, 43*, 333–361.

Tabor, N. J., Myers, T. S., & Michel, L. A. (2017). Sedimentologist's guide for recognition, description, and classification of paleosols. In K. E. Zeigler & W. G. Parker (Eds.), *Terrestrial Depositional Systems* (pp. 165–208). Elsevier.

Thomas, W. A., Gehrels, G. E., Sundell, K. E., Greb, S. F., Finzel, E. S., Clark, R. J., Malone, D. H., Hampton, B. A., & Romero, M. C. (2020). Detrital zircons and sediment dispersal in the eastern Midcontinent of North America. *Geosphere, 16*, 817–843.

Veevers, J. J., & Powell, C. . Mc. A. (1987). Late Paleozoic glacial episodes in Gondwanaland reflected in transgressive-regressive depositional sequences in Euramerica. *GSA Bulletin, 98*, 475–487.

Velde, B., & Vasseur, G. (1992). Estimation of the diagenetic smectite to illite transformation in time-temperature space. American Mineralogist, 77(9–10), 967–976.

Wanless, H. R. (1931). Pennsylvanian cycles in western Illinois. *Illinois State Geological Survey Bulletin, 60*, 179–193.

Wanless, H. R., & Shepard, F. P. (1936). Sea level and climatic changes related to late Paleozoic cycles. *Geological Society of America Bulletin, 47*, 1177–1206.

Warr, L. N. (2020). Recommended abbreviations for the names of clay minerals and associated phases. *Clay Minerals, 55*, 261–264.

Weller, J. M. (1930). Cyclical sedimentation of the Pennsylvanian period and Its significance. *The Journal of Geology, 38*, 97–135.

Weller, J. M. (1931). The conception of cyclical sedimentation during the Pennsylvanian period. *Illinois State Geological Survey Bulletin, 60*, 163–177.

Whelan, J. F., Cobb, J. C., & Rye, R. O. (1988). Stable isotope geochemistry of sphalerite and other mineral matter in coal beds of the Illinois and Forest City basins. *Economic Geology, 83*, 990–1007.

Willman, H. B., Atherton, E., Buschbach, T. C., Collinson, C., Frye, J. C., Hopkins, M. E., Lineback, J. A., & Simon, J. A. (1975). *Handbook of Illinois stratigraphy* (Vol. 95). Illinois State Geological Survey.

Worthen, A. H. (1866). *Economical geology of Illinois* (p. 541). Illinois Geological Survey.